Allometric scaling of thermal infrared emitted from UK cities and its relation to urban form

M. Abdulrasheed[1], A.R. MacKenzie[1, 2*], J. D. Whyatt[3], L. Chapman[1]

1. School of Geography, Earth and Environmental Science, University of Birmingham, Edgbaston, B15 2TT, Birmingham, UK

2. Birmingham Institute of Forest Research, University of Birmingham, Edgbaston, B15 2TT, Birmingham, UK

3. Lancaster Environment Centre, Lancaster University, Lancaster LA1 4YQ, UK.

* Corresponding author

ABSTRACT

As a result of differences in heat absorption and release between urban and rural landscapes, cities develop a climate different from their surroundings. The rise in global average surface temperature and high rates of urbanization, make it important to understand the energy balance of cities, including whether any energy-balance-related patterns emerge as a function of city size. In this study, images from the Moderate Resolution Imaging Spectro-radiometer (MODIS) satellite instrument, covering the period between 2000 and 2017, were sampled to examine the seasonal (winter and summer) night-time clear-sky upwelling long-wave energy for 35 UK cities. Total (area-summed) emitted energy per overpass per city is shown to correlate closely ($R^2 \geq 0.79$) with population on a log-log 'allometry' plot. The production of emitted energy from the larger cities is smaller than would be produced from a constellation of smaller cities housing the same population. The mean allometry slope over all overpasses sampled is 0.84±0.06, implying an 'economy (or parsimony) of scale' (i.e., a less-than-proportional increase) of about 21% (i.e. $100(2\text{-}10^{0.84\log(2)})$) for each doubling of city population. City area shows a very similar economy of scale, so that the scaling of night-time emitted energy with urban area is close to linear (1.0±0.05). This linearity with area indicates that the urban forms used in UK cities to accommodate people more efficiently per unit area as the urban population grows, do not have a large effect on the thermal output per unit area in each city. Although often appearing superficially very different, UK cities appear to be similar in terms of the components of urban form that dictate thermal properties. The difference between the scaling of the heat source and literature reports of the scaling of urban-rural air (or surface) temperature difference is very marked, suggesting that the other factors affecting the temperature difference act to decrease strongly its scaling with population.

HIGHLIGHTS

- MODIS was used to assess the clear-sky upwelling long-wave energy for thirty-five (35) large urban areas in Great Britain;
- A robust, less-than-proportional, scaling relationship between total urban population and total emitted energy demonstrates a thermal 'economy (or parsimony) of scale' with respect to population.

- The scaling relationships with population for city area and for emitted energy suggest a testable hypothesis regarding the similarity of energy budgets across urban areas of very different sizes.

Keywords: Urban Heat Island (UHI); Land Surface Temperature (LST); Allometry; Urban size and population; Geographic Information System (GIS); MODIS and Emitted energy

1.0 INTRODUCTION

Urbanization is accelerating across the world, especially in developing countries across Africa and Asia (Martins, 2000; Cohen, 2006). Current projections indicate that by 2050, the global urban population will increase by 2.4 billion, i.e., about half the current population of 4.22 billion (United Nation, 2019) (Seto et al., 2012; Buhaug and Urdal, 2013; Bremner et al., 2010; Bongaarts, 2009). The change of land surface characteristics caused by urbanisation leads, amongst other things, to changes in the local energy balance that must be taken into account when determining long-term temperature trends (Chrysanthou et al., 2014). This change in thermal climate in urban areas, leads to the urban heat island (UHI), which is the tendency of an urban area to have warmer near-surface air temperatures than its rural surroundings (Bornstein, 1968; Landsberg, 1981; Oke, 1995; Sheng et al., 2017). Related phenomena include: urban thermal plumes (Oke, 1995; Heaviside et al., 2015) and urban precipitation anomalies (Han et al., 2013).

Recent conceptual UHI models have emphasised the importance of different land uses within cities (Stewart and Oke, 2012; Tomlinson et al., 2012), highlighting the prospect that urban planning choices can be used to mitigate adverse urban climate trends (Davoudi, 2012; Davoudi, 2014). Implicit in most studies of UHI, from Howard (1818) on, is that local, one-dimensional (i.e., vertical), energy budgets for urban land uses, combine through the action of fluid stirring and mixing, to produce a three-dimensional dome of urban heating over a city — see, for example, the very widely reproduced cross-sections of UHI through an idealised city (e.g., Lemmon and Warren, 2004).

We hypothesise that gross changes in urban form affect the storage of solar heating as the size of cities increase. We focus on night-time, clear-sky, emitted long-wave energy as a primary measure of heat storage, and we use population as our measure of city size. We use an extensive property — total emitted energy (in Megawatts) per city per night — rather than intensive property such as temperature or emission per unit area, to permit direct comparisons with other extensive properties such as urban area, and to explore the extent to which the behaviour of intensive properties, particularly UHI, differ from the behaviour of the extensive properties.

1.1 Urban Form and urban heat

The urban form of a city is the result of its social, economic, and environmental context. We focus on UK cities in this study; further work will focus on a different setting in order to try and distinguish the general from that dependent on UK context (Abdulrasheed, 2020). A recognised system of UK urban planning mostly originates from the industrial revolution, prior to which most people lived and worked in the countryside (Inikori, 2002; CPRE, 2018). As industries grew, people migrated to towns and cities in search of better wages, opportunities, and livelihoods (Karp, 2013) leading to rapid growth in town and cities. Many decrees and ordinances were

issued to manage this growth, including, at the beginning of the 20th century, the Town Planning Act 1909, which was introduced to ensure that local authorities prepared schemes of town planning. This was followed by the Housing Act 1919, which required the design of houses to be approved by the Ministry of Health, and the Housing Act 1930, which required clearance of high-density 'slums', which were considered unsanitary (Carmon, 1999). The post-war 1940s was a period of uncertainty for the architects and town planners tasked with rebuilding Britain's bomb-damaged cities (Tsubaki, 2000; Ball and Maginn, 2005; Hollow, 2012). Residential rebuilding in this period often involved the replacement of low-rise private dwellings with fewer, but larger, high-rise public buildings (Carmon, 1999), sometimes with an intermediate period of low-rise prefabricated structures (Short, 1982). Cities across the UK such as Bristol, Coventry, Hull, Portsmouth, Southampton and Plymouth were very severely damaged during World War II (Hasegawa, 2013), and so were subject to significant post-war changes. For those neighbourhoods, which, by the 1960s and 1970s, had escaped slum clearance or destruction in wartime, the tendency was for renewal rather than replacement of low-rise and mid-rise residential buildings (Carmon, 1999). In the subsequent decades, and until the present day, a more laissez-faire approach has dominated, with renewal and replacement of housing and commercial buildings through private-public cost sharing of various kinds (Carmon, 1999; Hasegawa, 2013; Webb, 2018) .

Emerging in parallel, from the latter part of the nineteenth century and through the first part of the 20th century, was the Garden Cities movement, which advocated public health improvement by planning to build cities with more, and more accessible, green spaces, see e.g., (Burnett, 1986). This advocacy eventually led to the New Towns movement and New Towns Act 1946 (Goist, 1974; Rubin, 2009; Alexander, 2009; Tizot, 2018) which resulted in towns such as Telford, Letchworth and Milton Keynes. All the 20th-century housing and town planning policies in the UK led to notable changes in the urban form from the scale of individual dwellings, through neighbourhood scale land-use, to the patterns of use across whole urban areas.

The nature and patterns of urban form (i.e. building geometry, pervious surface fraction, building and tree densities, soil permeability etc.) determine the thermal characteristics of place. Such characteristics can be used to define local climate zones (LCZ)(Stewart et al., 2014), which may vary over time as a result of planned or unplanned changes. For example, slum clearance often re-shaped low-rise, close-packed, terraced housing into a sparse array of high-rise towers e.g., (Carmon, 1999). Suburban extension of cities replaced farm field (or, often, filled in parkland estates around large houses) with semi-detached two storey housing in wide boulevards (shifting from linear form to cul-de-sac mid-century). Infilling (building in what had previously been back gardens) became prominent towards the end of the 20th century (Whitehand and Whitehand, 1983).

As cities grow, green space — trees and vegetation — are replaced with grey space, i.e., buildings and transport and utility infrastructure. The magnitude and nature of the change is often sporadic and patchy, and results in a wide variety of urban forms (Morris, 1974; Hopkins, 2012). In terms of the surface energy balance, changing from rural to urban land results, in general, in the absorption of a higher fraction of incoming solar radiation and a decrease in the Bowen ratio (i.e., the ratio of sensible to latent heat emission) (Arnfield, 2003; Aguado and Burt, 2015). Energy absorption and emission at the ground surface is therefore a key driver of urban climate, strongly influencing the near surface air temperature and the radiant fluxes relevant for health effects (e.g., Basu and Samet, 2002; Middel and Krayenoff, 2019). Satellite based studies report thermal emission as land-surface temperature (or 'skin' temperature), from which surface

UHI intensity (SUHII) can be derived (e.g., Peng et al., 2012; Zhou D. et al., 2014; Zhou B. et al., 2017). In-situ sensing reports air temperature directly. Near-surface air temperature UHI and SUHII do not always correspond for a variety of physical reasons (Voogt and Oke, 1998; 2003; Arnfield, 2003; Schwarz et al., 2011; Sheng et al., 2017) but both are driven by absorption and emission of energy at the ground surface. The fundamental role of surface energy exchange motivates us to investigate how surface energy parameters vary for a set of cities of very different size and urban form, in order to understand this foundational driver of both the UHI and SUHII.

Buildings also slow the wind near the surface, retaining the heat released from vehicles and buildings (Golden, 2004; Arifwidodo and Tanaka, 2015). Energy removed from the mean wind is lost to the surfaces or transformed into turbulent kinetic energy, affecting the dissipation of scalars such as temperature and trace-gas pollutants e.g., (Belcher et al., 2003). Dense building arrangements decrease the sky-view factor (Chapman and Thornes, 2004; Grimmond, 2007; Yang et al., 2015). The net result of all these changes is the increased storage of heat, which is the root cause of the UHI effect. Increased heat storage can lead to a number of issues such as human health risk (Basu and Samet, 2002; Rosenzweig et al., 2011; Murray and Ebi, 2012; Smith et al., 2011; Patz et al., 2005; Hondula et al., 2015; Wouters et al., 2017; Krayenhoff et al., 2018; Middel and Krayenhoff, 2019), environmental hazard (e.g., Chapman and Thornes, 2006), and infrastructure failure (Chapman and Bell, 2018; Dawson et al., 2018), which themselves add heat to urban air and often require further energy consumption to offset (Li et al., 2015).

Researchers have long studied the effects of urban form on climate change, and the impacts of climate change on urban environment, as reviewed in (Mills, 2007) and (Seto et al., 2010). Urban planning responses to urban heat and climate change, including both mitigation and adaptation strategies, continue to evolve, especially with respect to sustainable urban development in cities (Jabareen, 2006 ; Rybski et al., 2017; Davoudi et al., 2009; Hendrickson et al., 2016; Castán Broto, 2017; Fujii et al., 2017). Urban climate adaptation focuses on reducing vulnerability and promoting resilience of people and properties (Amundsen et al., 2010; Carmin et al., 2012; Anguelovski et al., 2014). Microclimate planning and design modification to outdoor environment can also enhance thermal comfort, e.g., neighbourhood streets trees, green spaces and parks, (Brown, 2011; OECD, 2014). We expect that planning responses to urban heat will manifest in the relationship of urban form to city size.

1.2 Allometry and urban heat

Allometry is originally a concept from biology, relating morphological and physiological aspects of organism biology to some more easily measured parameters such as body mass (Schmidt-Nielsen, 1984; Gould, 1966; Lee, 1989; Small, 2012). Allometric approaches were introduced to urban studies (e.g. West and Brown, 2005; Naroll and Bertalanffy, 1956; Nordbeck, 1971) and used to model the relationship between a set of cities and the largest city within a geographical region (Small, 2012). Urban allometry studies have sought to elucidate decadal evolution of urbanized area (Lee, 1989; Longley et al., 1991), fractal spatial patterning (Chen, 2010), income inequality (Sarkar et al., 2018), and between urban form and growth (Bettencourt et al., 2007). Interpretations drawn from urban allometry include growth by innovation driven by economies of scale (Batty, 2008), and urban form as a hierarchy of clusters, (Bettencourt, 2013).

In general, for urban studies, allometric scaling relates aspects of urban material, energy, or economic flows to the size of cities as determined by their population (Bettencourt, 2013; Batty, 2008; Lee, 1989; Longley et al., 1992). Because it focuses on the relative rate of change of properties with size, referred to as 'scaling' below, allometry lends itself to comparative studies of properties of very different character (Bettencourt and West, 2010). In our previous study of air pollutant emissions and concentrations, we found it informative to compare the scaling of an intensive property (urban air concentrations) with the scaling of extensive properties (area-summed pollutant emissions and urban area) (MacKenzie et al., 2019).

Allometric scaling recognises that the many microscopic interactions within a complex system often collapse to a simple pattern (Cottineau et al., 2017). Scaling, therefore, allows us a synthesising perspective on cities (Batty, 2008), by searching for simple patterns without becoming overwhelmed by details of local context.

Allometric patterns, where they exist, conform closely to an equation of the form:

$$Y = \beta X^{\alpha} \qquad (1a)$$

The power law, equation (1a), describes a straight-line relationship between the X and Y variables when the function is plotted on a double logarithmic coordinate system, i.e.

$$log(Y) = log(\beta) + \alpha . log(X) \qquad (1b)$$

where $log(\beta)$ is a constant offset and α is the rate of relative growth (the allometric scaling factor or, simply, slope). Below, we will refer to α as defining the 'scaling' of Y with respect to X.

Using allometry, this study seeks a quantitative scaling relationship between population and clear-sky upwelling emitted energy, in order to determine whether and how the many detailed processes affecting this part of the urban energy budget combine at the city-scale. The study evaluates whether simplicity emerges from urban complexity with respect to emitted long-wave. We compare our findings on clear-sky upwelling long-wave to a classical result in the literature of urban heat islands.

The empirical relationship between the UHI and structure of a city arises from the fact that tall, close-packed, concrete and brick buildings store solar energy in day time and emit it at night more slowly than a flat surface (Duckworth and Sandberg, 1954). The thermal infrared energy emitted from a surface is acted on by wind and radiation transfer processes; structural elements of a city affecting wind and radiative transfer will therefore influence UHI (Oke, 1973). Since structural elements of cities are often laid out block by block, one approach to analysing a city is to determine its energy budget and surface temperature explicitly on a block-by-block basis (Terjung and Louie, 1974; Chandler, 1966). Land-use categories and urban morphology types offer useful approaches to determining modifications to the surface energy budget that will produce a nocturnal urban heat Island (Oke, 1981; Landsberg, 1981; Eliasson, 1996). Other urban climate studies focus on the effect of the urban surface at the neighbourhood scale, using land-use classifications to generalise results (e.g. Arnfield, 2003; Stewart and Oke, 2012). At city scale the number of studies are fewer: (Landsberg, 1981) for North American settlements; (Lee, 1993) for Korea; (Eagleman, 1974) for Kansas city; and (Oke and Maxwell, 1975) for Montreal and Vancouver.

Several studies in the urban climate literature offer an allometric perspective (Oke, 1982; Torok et al., 2001; Manoli et al., 2019), and many other comparative studies show that UHI or SUHII increases with some measure of the size of the city (e.g. Zhou B., et al., 2013; 2017; Schwarz and

Manceur, 2015) or focus on the largest cities because the UHI is assumed to be largest there (e.g., Peng et al., 2012; Zhou D., et al., 2014). Oke (1973; 1982) presented the relationship between a measure of maximum UHI ($\Delta T_{u\text{-}r}$(max)) and population for European settlements (fig.1) and supports the hypothesis that the canopy air temperature, $\Delta T_{u\text{-}r}$, is a function of city size, with the absolute UHI increasing by about 0.6 °C (i.e. $1.975.\log_{10}(2)$) for every doubling in population. Zhou et al. (2013) fitted a sigmoidal curve to the log-linear relationship of SUHII to urban area. The sigmoidal function is approximately linear for urban clusters with areas between 2 and 200 km^2 with SUHII increasing by ~0.3°C for an area doubling (Zhou et al., their Figure 2). Zhou et al. (2017) plot SUHII against $\log_e$(urban area) similarly to find a log-linear regression in which SUHII increases by about 0.4 °C (i.e. $0.55.\log_e(2)$) for an area doubling.

Fig S1 in the Supplementary Information presents the Oke (1973) data in a power-law log-log graph. Regressing on $\log_{10}(\Delta T_{u\text{-}r}(\max))$ gives more weight to the smaller cities, but a strong relationship is still found. The scaling of $\Delta T_{u\text{-}r}$ in Fig S1 is small, 0.11 ± 0.03, but significantly different from zero — and equivalent to an increase of just 8% (i.e. $100(10^{0.11.\log(2)}\text{-}1)$) in UHI for a population doubling. Using a similar log-log regression, Manoli et al. (2019) found a scaling with population of $\log_{10}$(SUHII) ranging between 0.15 and 0.24, equivalent to a maximum increase of 18% (i.e. $100(10^{0.24.\log(2)}\text{-}1)$) for a population doubling. Such relatively modest scalings with population have implications, such as that 'densification' of population into large urban centres presents a rather modest increased contribution of air temperature to thermal discomfort and associated health risk, at least to the extent that this can be gauged by the UHI of the 20th century city forms in Oke's (1973; 1982) sample.

Having identified the best-fit scaling relationship, the residual offset from this best-fit for any individual city is also informative (Bettencourt et al., 2010). The residual for any city on any night, $r_{j,k}$, is calculated as the vertical distance of the datum for that city to the best-fit line:

$$r_{j,k} = \log\left(Y_{j,k}\right) - \left\{log(\beta_k) + \alpha_k . log(X_j)\right\} \quad (2)$$

where $Y_{j,k}$ is the measured value of dependent variable (in our case, the summed emitted energy of city, j, on a given night, k), X_j is the population, of city j, and the parameters α_k and β_k define the allometric scaling relationship. In Oke's scaling data (Figs 1 and S1), the largest-magnitude residual is a large negative deviation (i.e. less heat island than expected) for the UK town of Reading (Oke, 1973).

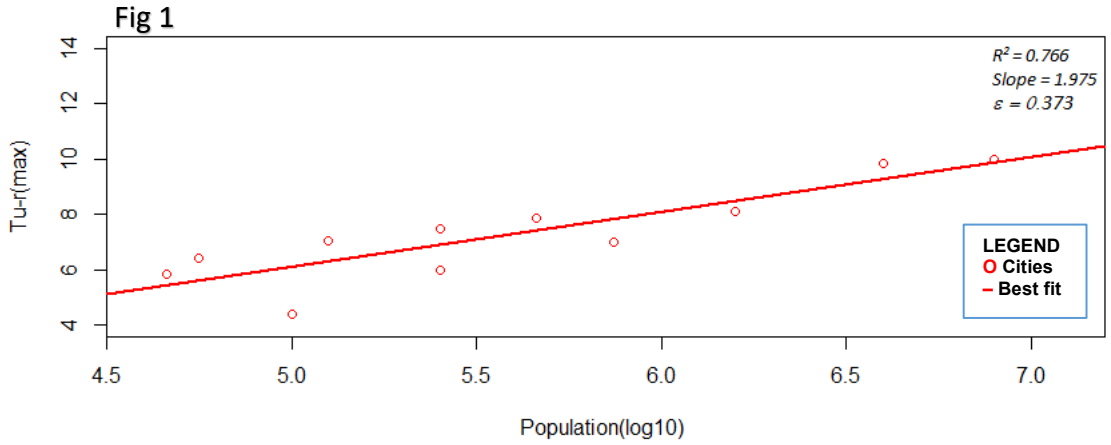

Fig.1. *Relation between maximum air temperature heat island intensity ($\Delta T_{u\text{-}r}$ (max), degrees Celsius) and population (P) for European Settlements (redrawn from Oke, 1982). Sources of $\Delta T_{u\text{-}r}$ (max) are literature and private communications dating from 1927 – 1972. It is not clear in Oke (1973; 1982) if the population data used is matched in time to the date for $\Delta T_{u\text{-}r}$ (max). Reported on the graph (top right) are the Coefficient of Determination (R^2) for the best-fit regression, the slope of the regression, and the error on the slope (ε).*

Since both the canopy air temperature UHI, and the surface temperature SUHII result from heat storage, the scaling of emitted energy (with population or urban area) will be an important contributor to the scaling of UHI and SUHII. When the observed scaling of emitted energy is larger than that for UHI or SUHII, other factors must be acting to dampen the overall scaling. Thus, this paper seeks to use allometric scaling, and importantly an interpretation of the residual offset, to inform the role of bulk urban morphology as a control for levels of urban heat.

2.0 METHODOLOGY

2.1 The study area

According to the Office for National Statistics (ONS), the population of UK as at 30th June 2016 is estimated to be 65,648,000, concentrated in urban areas in the southern half of the country (Figure 2a), and with a rate of increase of 0.8% (538,000) per annum (Office for National Statistics, 2017). The climate of UK is temperate, but variable, particularly because of altitude and distance from the coast (Figure 2b). Average temperature is 4°C January (winter) and 15°C in July (summer) (Kennedy et al., 2017; Briney, 2019). Mean climate data are shown in figure 2. This study focuses on thirty-five (35) large (area > 50km^2) settlements in the Great British mainland of the UK (see fig. 2a below and table S1 and fig S5 in supplementary section SI). Boundaries for the cities were extracted from medium scale digital map data (Meridian2; see Data Sources, below) produced by the Ordnance Survey (GB National Mapping Agency) and represent contiguous Developed Land Use Areas (DLUA) rather than administrative demarcations. UHI, SUHII, and urban allometry studies are sensitive to the choice of urban boundary and this should be borne in mind in the comparisons discussed below. The urban boundary used to define population in Oke (1973) is likely administrative; the urban cluster areas used in Zhou et al. (2013, 2017) are similar to our contiguous DLUA. Population counts

277 were retrieved from the Office of National Statistics (2017) at the lowest level of geographical
278 aggregation (output area) and attributed to the contiguous DLUAs.

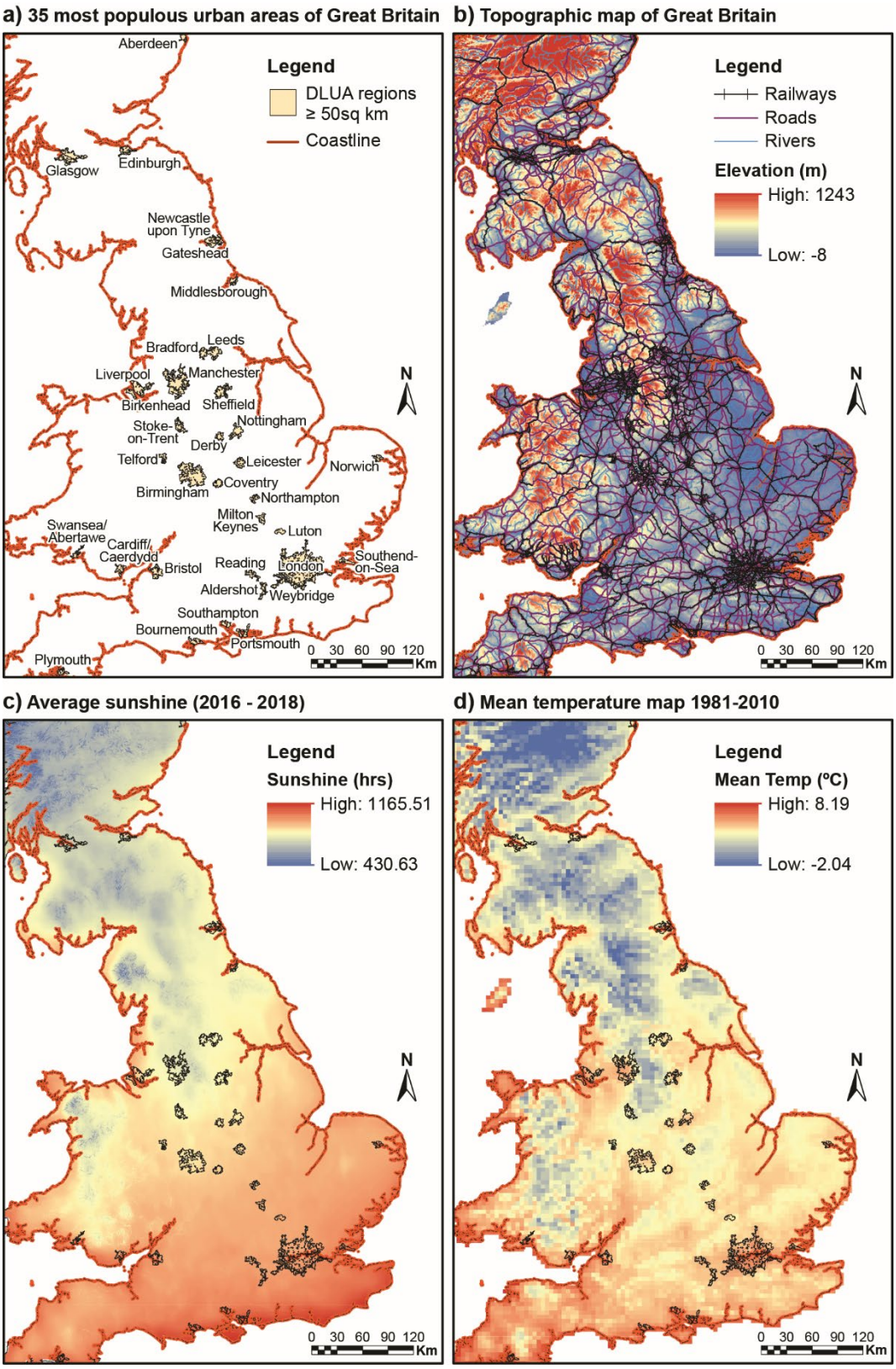

279

280 **Fig. 2** *(**a**) 35 most populous urban areas in Great Britain (urban boundaries are contiguous Developed*
281 *Land Use Areas from Meridian2 data); (**b**) Topographic map of central Great Britain with cities and*
282 *major roads; (**c**) Average Sunshine of central Great Britain; (**d**) Mean 2m Temperature map of central*

Great Britain. The data were sourced from Centre for Environmental Data Analysis (CEDA, 2011)*,* (SolarGIS, 2019)*, and ArcGIS tool were used to plot the maps.*

2.2 Data collection and analysis

This study uses MODIS/Terra V006 composite products (MOD11A1) – MODIS/Terra Land Surface Temperature and Emissivity Daily L3 Global 1km Grid SIN V006 (Wan et al., 2015). This product provides gridded, high resolution, cloud-cleared, quality-controlled and quality-assured data, and has accurate calibration in multiple thermal infrared bands designed for retrievals of Land Surface Temperature (LST) and atmospheric properties (Wan and Dozier, 1996; Wan et al., 2015). LST from MODIS are retrieved from clear sky observations at daytime and night-time with the aid of a generalized split-window algorithm (Wan and Dozier, 1996; Wan, 2008). It is established that satellite sensors looking in the nadir can oversample horizontal urban surfaces and undersample vertical surfaces (Voogt and Oke, 1998; Arnfield, 2003). This will tend to overemphasise both day-time heating and night-time cooling, the extent of which varies with the angle of view. Angle of view also affects the native spatial resolution of the satellite radiances; interpolation in the MOD11A1 processing pipeline brings the dataset to a uniform 1-km grid. The MOD11A1 dataset contains information on view angle but we have not implemented any further correction for off-nadir view geometries. For simplicity, only night-time overpasses (0130h local time) are considered for the present study.

Area-summed clear-sky night-time long-wave upwelling emitted energy (hereafter 'emitted energy') for mainland Great Britain was derived for selected days from 2000-2017. We interpret emitted energy in preference to LST because it gives proper weighting to radiance from the highest temperatures and provides a sum in physically meaningful units. The LST data used was selected to have as much clear sky over the region as possible. LST data for each pixel, *i*, within the city, *j*, on night, *k*, was converted to emitted energy, $\epsilon_{i,j}$ in W m^{-2}, using the Boltzmann law:

$$\epsilon_{i.j,k} = \sigma T_{i,j,k}^4 \qquad (3)$$

where, σ is the Stefan-Boltzmann constant = 5.67 x 10^{-8} W m^{-2} K^{-4}, and $T_{i,j,k}$ is the LST in Kelvin. The effect of varying surface emissivity is not taken into account. Area-summed emitted energy, $\langle E_j \rangle$ in MW, for each city on each night, was then calculated by summing the *p* unobscured land-surface pixels inside the city boundary:

$$\langle \mathrm{E}_{j,k} \rangle = \sum_{i=0}^{p} \epsilon_{i,j,k} \Delta a \qquad (4)$$

where Δa = 1 km^2 and the factor of 10^6 converting km^2 into m^2 is accommodated in the units of $\langle E_j \rangle$. A default 50% threshold of clear sky was set for each city on each image based on the assumption that adequate coverage of the study region can be achieved by sampling a large enough set of imagery. The threshold was implemented in ArcGIS simply by comparing the maximum area of each city as given by the Meridian dataset (Table S1) with the area inside the city containing valid LST (i.e. p.Δa) from the satellite dataset. The effect of using a 75% clear-sky threshold is discussed below.

2.3 Scaling Study Methodology

35 cities were selected for study using an arbitrary threshold of city area greater than 50 km^2, from which population and emitted energy were derived (table S3 in SI). Clear-sky nights were selected based on the prevalent synoptic meteorology (i.e., fog-free anticyclone conditions in the absence of fronts). A total of 28 nights was selected: 15 in winter (30 November – 28 February) and 13 in summer (1 June -31 August) in the period 2000 — 2017.

3.0 RESULTS

Area-summed emitted energy varies over 1.5 orders of magnitude for cities with populations ranging over 2 orders of magnitude (Figure 3a). Although the exact slope varies from night to night (Figure 3b), the tight log-log correlation is always present. Strong correlations are present on both summer and winter nights (table 1) with no obvious pattern, suggesting that scaling of emitted energy may not be as seasonal as the UHI or SUHII itself (cf. Zhou et al., 2013; Bechtel et al., 2019). The correlations suggest that population is a good predictor variable for total emitted energy, despite substantial differences in urban form of British cities. Figure 3b shows the plots for all dates sampled in this study. Slopes are similar, varying between 0.73±0.06 (13 December 2010; Table 1) and 0.92±0.09 (17 December 2011) and are ranked in Table 1 by their R^2 value when using a 50% cloud-free threshold. Standard error on the slope increases as R^2 decreases but there is no obvious trend in the value of the slope.

The derived regression equation for the averaged allometry over 28 nights is:

$$\log(\bar{Y}) = \log\left(\bar{\beta}\right) + \bar{\alpha}.\log\left(\overline{\langle E_j \rangle}\right), \quad (5)$$

where

$$\overline{\langle \mathrm{E}_j \rangle} = \frac{\sum_{k=0}^{n} E_{j,k}}{n}. \quad (6)$$

That is, $\overline{\langle E_j \rangle}$ is the average emitted energy (in MW) over all nights for city, j, and n is the number of nights = 28.

Although the two extreme values of the allometric slope are statistically different (i.e., the means are further apart than the sum of the standard errors, Table S3, Supplementary SI), Figure 3a does not show any clustering of the regression slopes in the sample. It is assumed, therefore, that, to a first approximation at least, the results indicate that a single overall allometric scaling of total emitted energy with population of 0.84±0.06 is plausible (fig.3b). If this assumption is justified, the variation observed in the regression slope must derive from difficult-to-quantify errors in the retrieval of the emitted energies, including the effect of partially obscured urban areas on the slope.

To test the impact of partial cloud obscuring, the analysis was repeated increasing the threshold for inclusion of an urban area in the analysis to 75% cloud-free (see table S3 and fig. S6 in supplementary SI). The scaling of emitted energy with population under this more stringent condition has a slope of 0.86±0.05 (Table S3 in Supplementary SI), which is, within error, indistinguishable from the mean slope from Table 1.

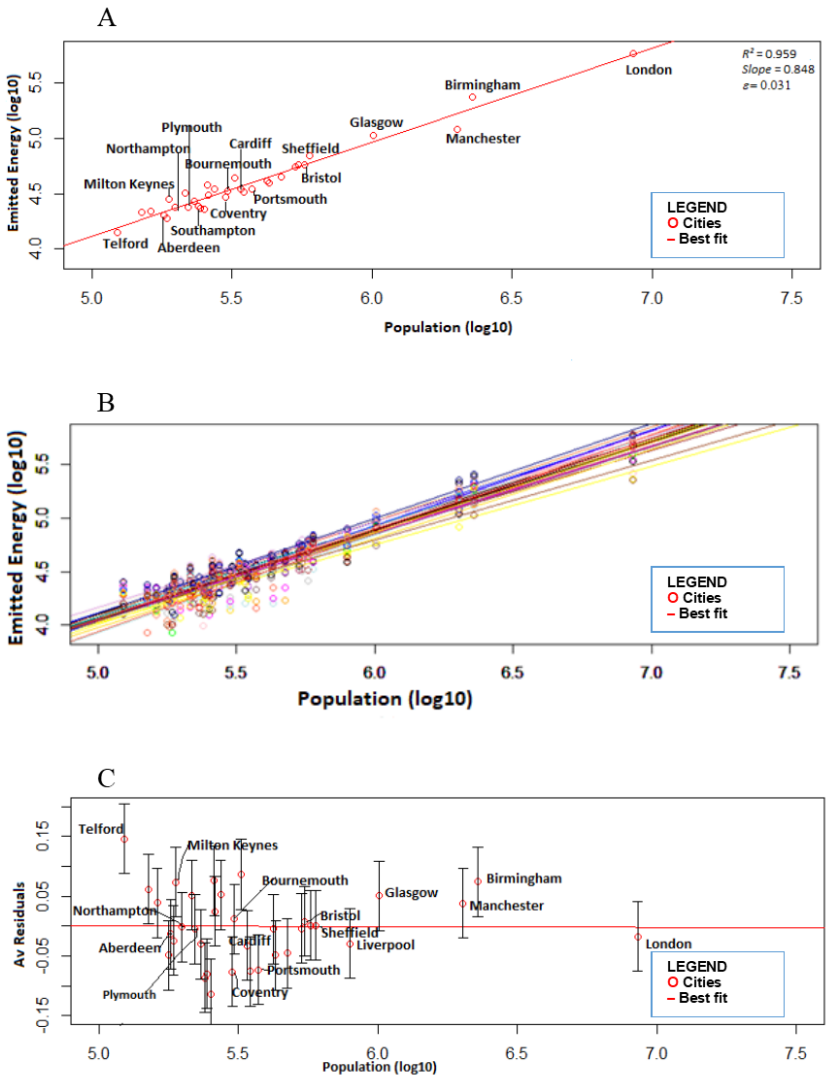

Fig. 3: (A) An example of allometric scaling of night-time emitted energy $Log_{10}(\langle E_j \rangle$, in MW) against urban population for the 35 largest cities in Great Britain. Reported on the graph (top right) are the Coefficient of Determination (R^2) for the best-fit regression, the slope of the regression, and the error on the slope (ε). (B) The ensemble of allometric relationships derived for the nights studied (Table 1). (C) Residual emitted energy (mean and standard deviation of $Log_{10}(\langle E_j \rangle$ in MW) for urban areas with respect to the allometric scalings shown in (B).

Table 1. *Night-time emitted energy for thirty-five (35) UK large Cities on selected summer and winter nights. Results are ranked by the strength (R^2) of the log-log correlation between emitted energy and population, for which the slope, and error on slope are reported at 50% cloud free pixels*

Rank	DATE	Number of CITIES	R^2	SLOPE (α)	ERROR ON SLOPE
1	13th Feb. 2017	26	0.97	0.86	0.03
2	15th Feb. 2016	25	0.96	0.85	0.03
3	06th Jun. 2000	33	0.96	0.85	0.03
4	22nd Feb. 2003	28	0.96	0.88	0.04

5	07th Jul. 2007	34	0.96	0.84	0.03
6	01st Jan. 2007	32	0.96	0.85	0.03
7	02nd Jan. 2017	35	0.94	0.84	0.04
8	26th Dec. 2009	24	0.93	0.81	0.05
9	27th Jun. 2010	32	0.93	0.80	0.04
10	16th Aug. 2016	35	0.92	0.89	0.04
11	29th Feb. 2000	21	0.92	0.83	0.05
12	01st Jan. 2012	24	0.92	0.89	0.06
13	30th Nov. 2016	20	0.92	0.86	0.06
14	13th Dec. 2010	17	0.92	0.73	0.06
15	28th Aug. 2001	25	0.91	0.88	0.06
16	30th Aug. 2005	22	0.90	0.82	0.06
17	20th Jan. 2009	18	0.88	0.83	0.08
18	09th Jul. 2006	34	0.88	0.88	0.06
19	20th Jan. 2011	22	0.88	0.74	0.06
20	08th Aug. 2012	25	0.88	0.83	0.06
21	05th Jan. 2005	34	0.88	0.80	0.05
22	10th Jun. 2003	27	0.87	0.81	0.06
23	13th Jul. 2002	28	0.87	0.77	0.06
24	03rd Aug. 2017	22	0.86	0.82	0.07
25	25th Feb. 2009	26	0.85	0.91	0.08
26	28th Aug. 2009	30	0.84	0.81	0.07
27	17th Dec. 2011	26	0.83	0.92	0.09
28	18th Feb. 2006	25	0.79	0.84	0.09
	Mean			**0.84**	**0.06**
	Median			**0.83**	

Table S4 (supplementary SI) tests the effect of a population threshold by comparing the correlations for cities with populations greater than 250,000 and greater than 500,000. The mean slope of the regression is not significantly different for both subsets of cities.

4.0 DISCUSSION

The findings from this study indicate that population is a good predictor variable for total emitted energy despite the differences in the urban form of UK cities. This study finds a much more significant scaling for upwelling clear-sky long-wave with population than was found for $\Delta T_{u\text{-}r}$ *(max)* by Oke (1973; 1982) (i.e., Fig. S1 in SI). Energy emitted from the surface is acted on by turbulent and radiative transfer processes, the net result of which is $\Delta T_{u\text{-}r}$ *(max)* (Oke, 1982). Although it is plausible that turbulent transfer processes scale with city size (as discussed in (MacKenzie et al., 2019)), it appears that the overall effect on the energy budget is to dampen very significantly the scaling of $\Delta T_{u\text{-}r}$ *(max)* compared to the scaling of emitted energy. The difference in the scalings of the heat source and the final temperature difference is very marked. Investigating this further will require a

386 detailed investigation of the scaling of each aspect of the urban energy budget, which is outside the
387 scope of the present study.

388 The scaling of emitted energy with population is very similar to that of total urban area with
389 population (Fig S2A in the SI). Hence, emitted energy varies linearly with urban area for the 35 cities
390 in our study (Fig S3), even though that area becomes increasingly densely populated as city
391 population increases. The implication is that, on average, there is no structural change of relevance
392 to the total emitted energy between a single city the size of London or ten cities each a tenth of the
393 area (i.e., roughly the size of Bristol). This quantitative scaling without qualitative structural change
394 may be consistent with Oke's 1973 study on city size and the urban heat Island, and with his study in
395 1981 on canyon geometry and the nocturnal urban heat Island, in which he cited Chandler's 1967
396 observation on the similarities of London and Leicester temperature on the same night, despite their
397 difference in size and population (Oke, 1973; 1981). Non-linearities may become more important
398 when smaller urban centres are included, as in the study of Zhou et al. (2013).

399 Further information pertaining to the urban form can be derived by inspection of the residuals, i.e.,
400 the distances of each urban area from the line of best fit (Fig 3c). We postulate that differences in
401 urban form across Great British cities will be evident in both the magnitude and sign of the residuals.
402 Firstly, however, we discount geographical and climate factors. Comparisons between mean
403 emitted-energy residuals and each of altitude, latitude, mean hours of sunshine, and mean annual
404 temperature for each city showed no significant correlations (see figs. S9, S10, S11 and S12 in
405 supplementary SI).

406 The magnitude of residual can be interpreted as the degree to which an individual city deviates
407 positively or negatively from the value expected for a city of its size (Bettencourt et al., 2010). For
408 the case of emitted thermal energy, positive anomalies correspond to cities with warmer surfaces
409 than expected and negative anomalies correspond to surfaces cooler than expected based on the
410 best-fit population-based allometry. There is a tendency for the magnitude of residuals to be larger
411 for the smaller urban areas (Fig 3c). For example, the residual for Telford is positive and about 4% of
412 its mean area-summed emission, whereas, for London, the residual is about 0.2% of the mean area-
413 summed emission.

414 The cities of Coventry and Plymouth, which were reconstructed post-war (Hasegawa et al., 2013)
415 have large negative residuals (-0.075 and -0.004 y-axis units ($\log_{10}(\langle E_j \rangle$ in MW)), Fig 3c), whereas the
416 New Town 'Garden Cities' of Milton Keynes and Telford both have large positive residuals (0.08 and
417 0.15 units). These unexpected results do not seem to arise from sampling issues affecting the overall
418 allometry because the residuals are robust for the various nights studied (variation bars in Fig 3c).
419 Instead, the results may arise from a greater area of impervious, low albedo, surface per person in
420 the lower density Garden Cities. Residuals for the area allometry for each city are reported in (table
421 S2 supplementary SI). Milton Keynes and Telford have large positive residuals compared to their
422 expected area (0.087 and 0.155 units, respectively), whilst Coventry and Plymouth have large
423 negative residuals (-0.056 and -0.050 units). So, the Garden cities emit more than expected for their
424 populations but spread that emission over a wider surface area than expected, whereas Coventry
425 and Plymouth emit much less than expected from their population but spread that emission over a
426 smaller-than-expected area.

427 Northampton, situated about 60 miles (97km) north-west of London and 45 miles (72km) south-east
428 of Birmingham, had a population of 212,100 at the 2011 census. Northampton is predominantly a
429 post-war settlement in which growth was limited until it was nominated as a New Town in 1968
430 (Whitehand and Whitehand, 1984). Its mean energy emission residual is close to zero, similar to

Bristol (fig. 3c), despite being radically different in terms of population and their histories of urban development. The residuals for urban area are also similar for Northampton and Bristol. However, Milton Keynes, the city closest to Northampton in population (table 1, supplementary SI), similarly situated (about 50 miles (80km) north-west of London), and also a classic post-war New Town, has a large positive mean emitted energy residual (fig 3c) and large positive area residual.

City configuration, street patterns and orientation, structure of buildings and density, and ultimately the intensity of human activities are key factors that determine thermal behaviour in the city. In summary, the residuals (fig. 3c) allow an assessment of the similarities and differences in emitted energy, relative to that expected by the best-fit line, for settlements of very different size.

5.0 CONCLUSION

This study aimed at evaluating the extent and rate of clear-sky emitted long-wave energy with population in the cities for MODIS/Terra V006 composite products (MOD11 A1). This was achieved by assessing the night-time emitted energy across cities in Great Britain for 28 night-time samples across summer and winter between 2000 and 2017. British cities show a strong and consistent sub-linear allometric scaling of total emitted energy with population. That is, there is a substantial 'economy (or parsimony) of scale' in terms of nocturnal heat production in British cities: the production from the larger cities is smaller than would be produced from a constellation of smaller cities housing the same population. This uniformity of scaling occurs despite of the obvious differences in architecture and urban form in settlements with Medieval centres (e.g. Aberdeen), predominantly commercial/military (e.g. Southampton) or residential (Bournemouth) coastal settlements, and post-second-world-war planned settlements (e.g., Milton Keynes).

The scaling of emitted energy with population is much larger than the scaling reported in the literature for the scaling of air temperature urban heat island (UHI) with population (Oke, 1973; Oke, 1982) or for the scaling of surface urban heat island intensity (SUHII) (Zhou et al., 2013; 2017). It is possible to compare these scalings even though emitted energy and UHI or SUHII have different units, because the logarithmic scaling produces a dimensionless slope quantifying relative changes (e.g., Bettencourt and West 2010). Since long-wave emissions from the relatively warm urban surface are the source of the nocturnal UHI and SUHII, turbulent and radiative transfer in the atmosphere must act to dampen significantly the scaling signal for heat island metrics. The concentration of population into larger urban areas, rather than spread out over more, smaller, cities, has only a marginal worsening effect on the risk to health arising from air temperature UHI but a much larger effect arising from radiant flux (cf., e.g., Middel and Krayenhoff, 2019).

The scaling of total emitted energy with population has a similar slope, within statistical error, as the scaling of urban area with population. This equality of scaling suggests that energy emitted per unit area averages out to be approximately the same everywhere in cities at the granularity of the current analysis. This 'emergent simplicity' in the scaling of emitted energy for urban areas of different sizes seems counter intuitive given our understanding of the role of urban form in heat storage and emission in the built environment (Arnfield and Grimmond, 1998; Nunez and Oke, 1977). Instead, the particularities of British urban form seem to manifest in the residuals for each city, i.e., the magnitude of the difference in emitted energy measured from that predicted by the best-fit line. As yet, we have not been able to find any simple rules that would allow us to predict the

size of the residual from its geographical context (including climate) or from its development history but we believe this merits further study.

Acknowledgements

We very gratefully acknowledge the substantial work of the referees and editor to improve the manuscript. ARMK and LC acknowledge support from the WM Air project of the Natural Environment Research Council (NE/S003487/1). MA gratefully acknowledges support from the Petroleum Technology Development Fund.

REFERENCES

Abdulrasheed, M., 2020. The Effect of Spatial Settlement Patterns on Urban Climatology. PhD Thesis, University of Birmingham, Birmingham, UK.

Aguado, E., Burt, J.E., 2015. Understanding Weather and Climate [WWW Document]. URL https://www.pearson.com/us/higher-education/product/Aguado-Understanding-Weather-and-Climate-7th-Edition/9780321987303.html (accessed 12.17.18).

Alexander, A., 2009. Britain's New Towns: Garden Cities to Sustainable Communities. Routledge.

Amundsen, H., Berglund, F., Westskog, H., 2010. Overcoming Barriers to Climate Change Adaptation—A Question of Multilevel Governance? Environ. Plan. C Gov. Policy 28, 276–289. https://doi.org/10.1068/c0941

Anguelovski, I., Chu, E., Carmin, J., 2014. Variations in approaches to urban climate adaptation: Experiences and experimentation from the global South. Glob. Environ. Change 27, 156–167. https://doi.org/10.1016/j.gloenvcha.2014.05.010

Arifwidodo, S.D., Tanaka, T., 2015. The Characteristics of Urban Heat Island in Bangkok, Thailand. Procedia - Soc. Behav. Sci., World Conference on Technology, Innovation and Entrepreneurship 195, 423–428. https://doi.org/10.1016/j.sbspro.2015.06.484

Arnfield, A.J., 2003. Two decades of urban climate research: a review of turbulence, exchanges of energy and water, and the urban heat island. Int. J. Climatol. 23, 1–26. https://doi.org/10.1002/joc.859

Arnfield, A.J., Grimmond, C.S.B., 1998. An urban canyon energy budget model and its application to urban storage heat flux modeling. Energy Build. 27, 61–68. https://doi.org/10.1016/S0378-7788(97)00026-1

Ball, M., Maginn, P.J., 2005. Urban Change and Conflict: Evaluating the Role of Partnerships in Urban Regeneration in the UK. Hous. Stud. 20, 9–28. https://doi.org/10.1080/0267303042000308705

Basu, R., Samet, J.M., 2002. Relation between Elevated Ambient Temperature and Mortality: A Review of the Epidemiologic Evidence. Epidemiol. Rev. 24, 190–202. https://doi.org/10.1093/epirev/mxf007

Batty, M., 2008. The Size, Scale, and Shape of Cities. Science 319, 769–771. https://doi.org/10.1126/science.1151419

Bechtel, B., Sismanidis, P., Voogt, J., Zhan, W., 2019. Seasonal Surface Urban Heat Island Analysis, in: 2019 Joint Urban Remote Sensing Event (JURSE). Presented at the 2019 Joint Urban Remote Sensing Event (JURSE), pp. 1–4. https://doi.org/10.1109/JURSE.2019.8808982

Belcher, S.E., Jerram, N., Hunt, J.C.R., 2003. Adjustment of a turbulent boundary layer to a canopy of roughness elements. J. Fluid Mech. 488, 369–398. https://doi.org/10.1017/S0022112003005019

Bettencourt, L.M.A., 2013. The Origins of Scaling in Cities. Science 340, 1438–1441. https://doi.org/10.1126/science.1235823

520 Bettencourt, L.M.A., Lobo, J., Helbing, D., Kühnert, C., West, G.B., 2007. Growth, innovation, scaling,
521 and the pace of life in cities. Proc. Natl. Acad. Sci. 104, 7301–7306.
522 https://doi.org/10.1073/pnas.0610172104
523 Bettencourt, L.M.A., Lobo, J., Strumsky, D., West, G.B., 2010. Urban Scaling and Its Deviations:
524 Revealing the Structure of Wealth, Innovation and Crime across Cities. PLOS ONE 5, e13541.
525 https://doi.org/10.1371/journal.pone.0013541
526 Bettencourt, L. and G. West, A unified theory of urban living. Nature, 2010. 467(7318): p. 912-913.
527 Bongaarts, J., 2009. Human population growth and the demographic transition. Philos. Trans. R. Soc.
528 B Biol. Sci. 364, 2985–2990. https://doi.org/10.1098/rstb.2009.0137
529 Bornstein, R.D., 1968. Observations of the Urban Heat Island Effect in New York City. J. Appl.
530 Meteorol. 7, 575–582. https://doi.org/10.1175/1520-
531 0450(1968)007<0575:OOTUHI>2.0.CO;2
532 Bremner, J., Frost, A., Haub, C., Mather, M., Ringheim, K., Zuehlke, E., 2010. World population
533 highlights: Key findings from PRB's 2010 world population data sheet. Popul. Bull. 65, 1–12.
534 Briney, A., 2019. How the United Kingdom Became an Island Nation [WWW Document]. ThoughtCo.
535 URL https://www.thoughtco.com/geography-of-the-united-kingdom-1435710 (accessed
536 9.4.19).
537 Brown, R., 2011. Ameliorating the effects of climate change: Modifying microclimates through
538 design. Landsc. Urban Plan. - Landsc. URBAN PLAN 100, 372–374.
539 https://doi.org/10.1016/j.landurbplan.2011.01.010
540 Buhaug, H., Urdal, H., 2013. An urbanization bomb? Population growth and social disorder in cities.
541 Glob. Environ. Change 23, 1–10. https://doi.org/10.1016/j.gloenvcha.2012.10.016
542 Burnett, J., 1986. Social History of Housing by Burnett - AbeBooks [WWW Document]. URL
543 https://www.abebooks.co.uk/book-search/title/social-history-of-housing/author/burnett/
544 (accessed 9.28.19).
545 Carmin, J., Anguelovski, I., Roberts, D., 2012. Urban Climate Adaptation in the Global South: Planning
546 in an Emerging Policy Domain. J. Plan. Educ. Res. 32, 18–32.
547 https://doi.org/10.1177/0739456X11430951
548 Carmon, N., 1999. Three generations of urban renewal policies: analysis and policy implications.
549 Geoforum 30, 145–158. https://doi.org/10.1016/S0016-7185(99)00012-3
550 Castán Broto, V., 2017. Urban Governance and the Politics of Climate change. World Dev. 93, 1–15.
551 https://doi.org/10.1016/j.worlddev.2016.12.031
552 CEDA, 2011. CEDA Data Server, Index of /badc/ukcp09/data/gridded-land-obs/gridded-land-obs-
553 averages-5km/grid/netcdf/mean-temperature/ [WWW Document]. URL
554 http://data.ceda.ac.uk/badc/ukcp09/data/gridded-land-obs/gridded-land-obs-averages-
555 5km/grid/netcdf/mean-temperature/ (accessed 10.2.18).
556 Chandler, T.J., 1966. The climate of London. By T. J. Chandler. London (Hutchinson), 1965. Pp. 292 :
557 86 Figures; 98 Tables; 5 Appendix Tables. £3. 10s. 0d. Q. J. R. Meteorol. Soc. 92, 320–321.
558 https://doi.org/10.1002/qj.49709239230
559 Chapman, L., Bell, S.J., 2018. High-Resolution Monitoring of Weather Impacts on Infrastructure
560 Networks Using the Internet of Things. Bull. Am. Meteorol. Soc. 99, 1147–1154.
561 https://doi.org/10.1175/BAMS-D-17-0214.1
562 Chapman, L., Thornes, J.E., 2006. A geomatics-based road surface temperature prediction model. Sci.
563 Total Environ., Urban Environmental Research in the UK: The Urban Regeneration and the
564 Environment (NERC URGENT) Programme and associated studies. 360, 68–80.
565 https://doi.org/10.1016/j.scitotenv.2005.08.025
566 Chapman, L., Thornes, J.E., 2004. Real-Time Sky-View Factor Calculation and Approximation: Journal
567 of Atmospheric and Oceanic Technology: Vol 21, No 5 [WWW Document]. URL
568 https://journals.ametsoc.org/doi/full/10.1175/1520-
569 0426%282004%29021%3C0730%3ARSFCAA%3E2.0.CO%3B2 (accessed 8.21.19).

570 Chen, Y., 2010. Characterizing Growth and Form of Fractal Cities with Allometric Scaling Exponents
571 [WWW Document]. Discrete Dyn. Nat. Soc. https://doi.org/10.1155/2010/194715
572 Chrysanthou, A., van der Schrier, G., van den Besselaar, E.J.M., Klein Tank, A.M.G., Brandsma, T.,
573 2014. The effects of urbanization on the rise of the European temperature since 1960.
574 Geophys. Res. Lett. 41, 7716–7722. https://doi.org/10.1002/2014GL061154
575 Clinton, N., Gong, P., 2013. MODIS detected surface urban heat islands and sinks: Global locations
576 and controls. Remote Sens. Environ. 134, 294–304.
577 https://doi.org/10.1016/j.rse.2013.03.008
578 Cohen, B., 2006. Urbanization in developing countries: Current trends, future projections, and key
579 challenges for sustainability. Technol. Soc., Sustainable Cities 28, 63–80.
580 https://doi.org/10.1016/j.techsoc.2005.10.005
581 Cottineau, C., Hatna, E., Arcaute, E., Batty, M., 2017. Diverse cities or the systematic paradox of
582 Urban Scaling Laws. Comput. Environ. Urban Syst., Spatial analysis with census data:
583 emerging issues and innovative approaches 63, 80–94.
584 https://doi.org/10.1016/j.compenvurbsys.2016.04.006
585 CPRE, 2018. Campaign to Protect Rural England | 38 Degrees [WWW Document]. URL
586 https://you.38degrees.org.uk/partnerships/campaign-to-protect-rural-england (accessed
587 9.28.19).
588 Davoudi, S., 2014. Climate Change, Securitisation of Nature, and Resilient Urbanism. Environ. Plan. C
589 Gov. Policy 32, 360–375. https://doi.org/10.1068/c12269
590 Davoudi, S., 2012. Climate Risk and Security: New Meanings of “the Environment” in the English
591 Planning System. Eur. Plan. Stud. 20, 49–69. https://doi.org/10.1080/09654313.2011.638491
592 Davoudi, S., Crawford, J., Mehmood, A., 2009. Planning for climate change: strategies for mitigation
593 and adaptation for spatial planners. Earthscan.
594 Dawson, R.J., Thompson, D., Johns, D., Wood, R., Darch, G., Chapman, L., Hughes, P.N., Watson,
595 G.V.R., Paulson, K., Bell, S., Gosling, S.N., Powrie, W., Hall, J.W., 2018. A systems framework
596 for national assessment of climate risks to infrastructure. Philos. Transact. A Math. Phys.
597 Eng. Sci. 376. https://doi.org/10.1098/rsta.2017.0298
598 Duckworth, F.S., Sandberg, J.S., 1954. The Effect of Cities upon Horizontal and Vertical Temperature
599 Gradients. Bull. Am. Meteorol. Soc. 35, 198–207.
600 Eagleman, J.R., 1974. A comparison of urban climatic modifications in three cities. Atmospheric
601 Environ. 1967 8, 1131–1142. https://doi.org/10.1016/0004-6981(74)90047-X
602 Earthdata, 2017. LP DAAC - Homepage [WWW Document]. URL https://lpdaac.usgs.gov/ (accessed
603 10.16.19).
604 Eliasson, I., 1996. Urban nocturnal temperatures, street geometry and land use. Atmos. Environ.,
605 Conference on the Urban Thermal Environment Studies in Tohwa 30, 379–392.
606 https://doi.org/10.1016/1352-2310(95)00033-X
607 Fujii, H., Iwata, K., Managi, S., 2017. How do urban characteristics affect climate change mitigation
608 policies? J. Clean. Prod. 168, 271–278. https://doi.org/10.1016/j.jclepro.2017.08.221
609 Fuller, R.A., Gaston, K.J., 2009. The scaling of green space coverage in European cities. Biol. Lett. 5,
610 352–355. https://doi.org/10.1098/rsbl.2009.0010
611 Goist, P.D., 1974. Patrick Geddes and the City. J. Am. Inst. Plann. 40, 31–37.
612 https://doi.org/10.1080/01944367408977444
613 Golden, J.S., 2004. The Built Environment Induced Urban Heat Island Effect in Rapidly Urbanizing
614 Arid Regions – A Sustainable Urban Engineering Complexity. Environ. Sci. 1, 321–349.
615 https://doi.org/10.1080/15693430412331291698
616 Gould, S.J., 1966. Allometry and Size in Ontogeny and Phylogeny. Biol. Rev. 41, 587–638.
617 https://doi.org/10.1111/j.1469-185X.1966.tb01624.x
618 Grimmond, S., 2007. Urbanization and global environmental change: local effects of urban warming.
619 Geogr. J. 173, 83–88. https://doi.org/10.1111/j.1475-4959.2007.232_3.x

Han, J.-Y., Baik, J.-J., Lee, H., 2013. Urban impacts on precipitation. Asia-Pac. J. Atmospheric Sci. 50. https://doi.org/10.1007/s13143-014-0016-7
Hasegawa, J., 2013. The attitudes of the Ministry of Town and Country Planning towards blitzed cities in 1940s Britain. Plan. Perspect. 28, 271–289. https://doi.org/10.1080/02665433.2013.737712
Heaviside, C., Cai, X.-M., Vardoulakis, S., 2015. The effects of horizontal advection on the urban heat island in Birmingham and the West Midlands, United Kingdom during a heatwave. Q. J. R. Meteorol. Soc. 141, 1429–1441. https://doi.org/10.1002/qj.2452
Hendrickson, T.P., Nikolic, M., Rakas, J., 2016. Selecting climate change mitigation strategies in urban areas through life cycle perspectives. J. Clean. Prod. 135, 1129–1137. https://doi.org/10.1016/j.jclepro.2016.06.075
Hollow, M., 2012. 'Utopian urges: visions for reconstruction in Britain, 1940–1950.' Plan. Perspect. 27, 569–585. https://doi.org/10.1080/02665433.2012.705126
Hondula, D.M., Balling, R.C., Vanos, J.K., Georgescu, M., 2015. Rising Temperatures, Human Health, and the Role of Adaptation. Curr. Clim. Change Rep. 1, 144–154. https://doi.org/10.1007/s40641-015-0016-4
Hoornweg, D., Lorraine Sugar, Claudia Lorena Trejos Gómez, 2011. Cities and greenhouse gas emissions: moving forward. Environ. Urban. 23, 207–227. https://doi.org/10.1177/0956247810392270
Hopkins, M. I. W., 2012. The ecological significance of urban fringe belts, Urban Morphology, 16, 41-54.
Howard, L., 1818: *The Climate of London, Vol.1*, London.
Inikori, J.E., 2002. A Historiography of the First Industrial Revolution [WWW Document]. Afr. Ind. Revolut. Engl. Study Int. Trade Econ. Dev. https://doi.org/10.1017/CBO9780511583940.004
Jabareen, Y.R., 2006. Sustainable Urban Forms: Their Typologies, Models, and Concepts. J. Plan. Educ. Res. 26, 38–52. https://doi.org/10.1177/0739456X05285119
Karp, M., 2013. A Very Old Book: The Case for Eric Hobsbawm's Age of Revolution. The Junto. URL https://earlyamericanists.com/2013/02/07/a-very-old-book-the-case-for-eric-hobsbawms-age-of-revolution/ (accessed 12.29.18).
Kennedy, J., Dunn, R., McCarthy, M., Titchner, H., Morice, C., 2017. Global and regional climate in 2016. Weather 72, 219–225. https://doi.org/10.1002/wea.3042
Krayenhoff, E.S., Moustaoui, M., Broadbent, A.M., Gupta, V., Georgescu, M., 2018. Diurnal interaction between urban expansion, climate change and adaptation in US cities. Nat. Clim. Change 8, 1097. https://doi.org/10.1038/s41558-018-0320-9
Landsberg, H.E., 1981. The Urban Climate. Academic Press.
Lee, H.-Y., 1993. An application of NOAA AVHRR thermal data to the study of urban heat islands. Atmospheric Environ. Part B Urban Atmosphere 27, 1–13. https://doi.org/10.1016/0957-1272(93)90041-4
Lee, Y., 1989. An Allometric Analysis of the US Urban System: 1960 – 80. Environ. Plan. Econ. Space 21, 463–476. https://doi.org/10.1068/a210463
Lemmen, D. S., and F. J. Warren (eds.), 2004. Climate Change Impacts and Adaptation: A Canadian Perspective. Climate Change Impacts and Adaptation Program, Natural Resources Canada. Available at https://cfs.nrcan.gc.ca/publications?id=27428
Li, M., Shi, J., Guo, J., Cao, J., Niu, J., Xiong, M., 2015. Climate Impacts on Extreme Energy Consumption of Different Types of Buildings. PLOS ONE 10, e0124413. https://doi.org/10.1371/journal.pone.0124413
Li, R., Dong, L., Zhang, J., Wang, X., Wang, W.-X., Di, Z., Stanley, H.E., 2017. Simple spatial scaling rules behind complex cities. Nat. Commun. 8, 1841. https://doi.org/10.1038/s41467-017-01882-w

669 Longley, P., Batty, M., Shepherd, J., Sadler, G., 1992. Do Green Belts Change the Shape of Urban
670 Areas? A Preliminary Analysis of the Settlement Geography of South East England. Reg. Stud.
671 26, 437–452. https://doi.org/10.1080/00343409212331347101
672 Longley, P.A., Batty, M., Shepherd, J., 1991. The Size, Shape and Dimension of Urban Settlements.
673 Trans. Inst. Br. Geogr. 16, 75–94. https://doi.org/10.2307/622907
674 MacKenzie, A.R., Whyatt, J.D., Barnes, M.J., Davies, G., Hewitt, C.N., 2019. Urban form strongly
675 mediates the allometric scaling of airshed pollution concentrations. Environ. Res. Lett. 14,
676 124078. https://doi.org/10.1088/1748-9326/ab50e3
677 Manoli, G., Fatichi, S., Schläpfer, M., Yu, K., Crowther, T.W., Meili, N., Burlando, P., Katul, G.G., Bou-
678 Zeid, E., 2019. Magnitude of urban heat islands largely explained by climate and population.
679 Nature 573, 55–60. https://doi.org/10.1038/s41586-019-1512-9
680 Martins, P.B., 2000. Urbanizing World [WWW Document]. URL
681 http://www.prb.org/Publications/Reports/2000/AnUrbanizingWorldPDF619KB.aspx
682 (accessed 11.26.17).
683 Middel, A. and E. S. Krayenhoff, 2019. Micrometeorological determinants of pedestrian thermal
684 exposure during record-breaking heat in Tempe, Arizona: Introducing the MaRTy
685 observational platform. Sci. Tot. Environ. 687: 137-151.
686 https://www.sciencedirect.com/science/article/pii/S0048969719326531
687 Mills, G., 2007. Cities as agents of global change. Int. J. Climatol. 27, 1849–1857.
688 https://doi.org/10.1002/joc.1604
689 Morris, A. E. J., 1974. History of Urban Form, Geo. Godwin, London.
690 Murray, V., Ebi, K.L., 2012. IPCC Special Report on Managing the Risks of Extreme Events and
691 Disasters to Advance Climate Change Adaptation (SREX). J Epidemiol Community Health 66,
692 759–760. https://doi.org/10.1136/jech-2012-201045
693 Naroll, R.S., Bertalanffy, L. von, 1956. The principle of allometry in biology and the social sciences.
694 Gen. Syst. Yearb.
695 Nordbeck, S., 1971. Urban Allometric Growth. Geogr. Ann. Ser. B Hum. Geogr. 53, 54–67.
696 https://doi.org/10.2307/490887
697 Nunez, M., Oke, T.R., 1977. The Energy Balance of an Urban Canyon. J. Appl. Meteorol. 16, 11–19.
698 https://doi.org/10.1175/1520-0450(1977)016<0011:TEBOAU>2.0.CO;2
699 OECD, 2014. OECD and Bloomberg Philanthropies: Cities and Climate... - Google Scholar [WWW
700 Document]. URL
701 https://scholar.google.com/scholar_lookup?title=Cities%20and%20Climate%20Change%3A
702 %20National%20Governments%20Enabling%20Local%20Action&publication_year=2014&au
703 thor=OECD (accessed 4.27.19).
704 Office for National Statistics, 2017. Population estimates - Office for National Statistics [WWW
705 Document]. URL
706 https://www.ons.gov.uk/peoplepopulationandcommunity/populationandmigration/populati
707 onestimates (accessed 12.9.17).
708 Oke, T.R., 1995. The Heat Island of the Urban Boundary Layer: Characteristics, Causes and Effects, in:
709 Wind Climate in Cities, NATO ASI Series. Springer, Dordrecht, pp. 81–107.
710 https://doi.org/10.1007/978-94-017-3686-2_5
711 Oke, T.R., 1982. The energetic basis of the urban heat island. Q. J. R. Meteorol. Soc. 108, 1–24.
712 https://doi.org/10.1002/qj.49710845502
713 Oke, T.R., 1981. Canyon geometry and the nocturnal urban heat island: Comparison of scale model
714 and field observations. J. Climatol. 1, 237–254. https://doi.org/10.1002/joc.3370010304
715 Oke, T.R., 1973. City size and the urban heat island. Atmospheric Environ. 1967 7, 769–779.
716 https://doi.org/10.1016/0004-6981(73)90140-6
717 Oke, T.R., Maxwell, G.B., 1975. Urban heat island dynamics in Montreal and Vancouver. Atmospheric
718 Environ. 1967 9, 191–200. https://doi.org/10.1016/0004-6981(75)90067-0

719 Patz, J.A., Campbell-Lendrum, D., Holloway, T., Foley, J.A., 2005. Impact of regional climate change
720 on human health. Nature 438, 310–317. https://doi.org/10.1038/nature04188
721 Peng, S., Piao, S., Ciais, P., Friedlingstein, P., Ottle, C., Bréon, F.-M., Nan, H., Zhou, L., Myneni, R.B.,
722 2012. Surface Urban Heat Island Across 419 Global Big Cities. Environ. Sci. Technol. 46, 696–
723 703. https://doi.org/10.1021/es2030438
724 Rosenzweig, C., Solecki, W.D., Hammer, S.A., Mehrotra, S., 2011. Climate Change and Cities: First
725 Assessment Report of the Urban Climate Change Research Network. Cambridge University
726 Press.
727 Rubin, N.H., 2009. The changing appreciation of Patrick Geddes: a case study in planning history.
728 Plan. Perspect. 24, 349–366. https://doi.org/10.1080/02665430902933986
729 Rybski, D., Reusser, D.E., Winz, A.-L., Fichtner, C., Sterzel, T., Kropp, J.P., 2017. Cities as nuclei of
730 sustainability? Environ. Plan. B Urban Anal. City Sci. 44, 425–440.
731 https://doi.org/10.1177/0265813516638340
732 Sarkar, S., Phibbs, P., Simpson, R., Wasnik, S., 2018. The scaling of income distribution in Australia:
733 Possible relationships between urban allometry, city size, and economic inequality. Environ.
734 Plan. B Urban Anal. City Sci. 45, 603–622. https://doi.org/10.1177/0265813516676488
735 Schmidt-Nielsen, K., 1984. Scaling: Why is Animal Size So Important? Cambridge University Press.
736 Schwarz, N., Lautenbach, S., Seppelt, R., 2011. Exploring indicators for quantifying surface urban
737 heat islands of European cities with MODIS land surface temperatures. Remote Sens.
738 Environ. 115, 3175–3186. https://doi.org/10.1016/j.rse.2011.07.003
739 Seto, K.C., Güneralp, B., Hutyra, L.R., 2012. Global forecasts of urban expansion to 2030 and direct
740 impacts on biodiversity and carbon pools. Proc. Natl. Acad. Sci. 109, 16083–16088.
741 https://doi.org/10.1073/pnas.1211658109
742 Seto, K.C., Sánchez-Rodríguez, R., Fragkias, M., 2010. The New Geography of Contemporary
743 Urbanization and the Environment. Annu. Rev. Environ. Resour. 35, 167–194.
744 https://doi.org/10.1146/annurev-environ-100809-125336
745 Sheng, L., Tang, X., You, H., Gu, Q., Hu, H., 2017. Comparison of the urban heat island intensity
746 quantified by using air temperature and Landsat land surface temperature in Hangzhou,
747 China. Ecol. Indic. 72, 738–746. https://doi.org/10.1016/j.ecolind.2016.09.009
748 Short, J.R., 1982. Housing in Britain: The Post-war Experience. Routledge, London ; New York.
749 Small, C.G., 2012. The Statistical Theory of Shape. Springer Science & Business Media.
750 Smith, C.L., Webb, A., Levermore, G.J., Lindley, S.J., Beswick, K., 2011. Fine-scale spatial temperature
751 patterns across a UK conurbation. Clim. Change 109, 269–286.
752 https://doi.org/10.1007/s10584-011-0021-0
753 SolarGIS, 2019. Global Solar Atlas [WWW Document]. URL
754 https://globalsolaratlas.info/support/release-notes (accessed 1.25.20).
755 Stewart, I.D., Oke, T.R., 2012. Local Climate Zones for Urban Temperature Studies. Bull. Am.
756 Meteorol. Soc. 93, 1879–1900. https://doi.org/10.1175/BAMS-D-11-00019.1
757 Stewart, I.D., Oke, T.R., Krayenhoff, E.S., 2014. Evaluation of the 'local climate zone' scheme using
758 temperature observations and model simulations. Int. J. Climatol. 34, 1062–1080.
759 https://doi.org/10.1002/joc.3746
760 Terjung, W.H., Louie, S.S.-F., 1974. A Climatic Model of Urban Energy Budgets. Geogr. Anal. 6, 341–
761 367. https://doi.org/10.1111/j.1538-4632.1974.tb00519.x
762 Tizot, J.-Y., 2018. Ebenezer Howard's Garden City Idea and the Ideology of Industrialism. Cah.
763 Victoriens Edouardiens 87. https://doi.org/10.4000/cve.3605
764 Tomlinson, C.J., Chapman, L., Thornes, J.E., Baker, C.J., 2012. Derivation of Birmingham's summer
765 surface urban heat island from MODIS satellite images. Int. J. Climatol. 32, 214–224.
766 https://doi.org/10.1002/joc.2261
767 Torok, S. J., J. G. Morris, C. Skinner, and N. Plummer, 2001. Urban heat island features of
768 southeast Australian towns. Aust. Meteorol. Mag., 50, 1–13.

Tsubaki, T., 2000. Planners and the public: British popular opinion on housing during the second world war. Contemp. Br. Hist. 14, 81–98. https://doi.org/10.1080/13619460008581573
Voogt, J. A., and T. R. Oke, 1998. Effects of urban surface geometry on remotely-sensed surface temperature. Int. J. Remote Sensing, 19(5), 895-920.
Voogt, J. A., and T. R. Oke, 2003. Thermal remote sensing of urban climates. Remote Sensing of Environment, 86(3), 370-384.Wan, Z., 2008. New refinements and validation of the MODIS Land-Surface Temperature/Emissivity products. Remote Sens. Environ. 112, 59–74. https://doi.org/10.1016/j.rse.2006.06.026
Wan, Z., Dozier, J., 1996. A generalized split-window algorithm for retrieving land-surface temperature from space. IEEE Trans. Geosci. Remote Sens. 34, 892–905. https://doi.org/10.1109/36.508406
Wan, Z., S. Hook, G. Hulley, 2015. MOD11A1 MODIS/Terra Land Surface Temperature/Emissivity Daily L3 Global 1km SIN Grid V006. Distributed by NASA EOSDIS Land Processes DAAC, https://doi.org/10.5067/MODIS/MOD11A1.006. Accessed 2020-05-19.
Webb, M.S., 2018. Local responses to the protection of medieval buildings and archaeology in British post-war town reconstruction: Southampton and Coventry. Urban Hist. 45, 635–659. https://doi.org/10.1017/S0963926818000019
West, G.B., Brown, J.H., 2005. The origin of allometric scaling laws in biology from genomes to ecosystems: towards a quantitative unifying theory of biological structure and organization. J. Exp. Biol. 208, 1575–1592. https://doi.org/10.1242/jeb.01589
Whitehand, J.W.R., Whitehand, S.M., 1983. The Study of Physical Change in Town Centres: Research Procedures and Types of Change. Trans. Inst. Br. Geogr. 8, 483–507. https://doi.org/10.2307/621964
Whitehand, J.W.R., Whitehand, S.M.R., 1984. The Physical Fabric of Town Centres: The Agents of Change. Trans. Inst. Br. Geogr. 9, 231. https://doi.org/10.2307/622170
Wouters, H., De Ridder, K., Poelmans, L., Willems, P., Brouwers, J., Hosseinzadehtalaei, P., Tabari, H., Vanden Broucke, S., van Lipzig, N.P.M., Demuzere, M., 2017. Heat stress increase under climate change twice as large in cities as in rural areas: A study for a densely populated midlatitude maritime region. Geophys. Res. Lett. 44, 8997–9007. https://doi.org/10.1002/2017GL074889
Yang, J., Wong, M.S., Menenti, M., Nichol, J., 2015. Modeling the effective emissivity of the urban canopy using sky view factor. ISPRS J. Photogramm. Remote Sens. 105, 211–219. https://doi.org/10.1016/j.isprsjprs.2015.04.006
Yow, D.M., 2007. Urban Heat Islands: Observations, Impacts, and Adaptation. Geogr. Compass 1, 1227–1251. https://doi.org/10.1111/j.1749-8198.2007.00063.x
Zhou, B., Lauwaet, D., Hooyberghs, H., De Ridder, K., Kropp, J., Rybski, D., 2016. Assessing Seasonality in the Surface Urban Heat Island of London. J. Appl. Meteorol. Climatol. 55, 493–505. https://doi.org/10.1175/JAMC-D-15-0041.1
Zhou, B., Rybski, D., Kropp, J.P., 2013. On the statistics of urban heat island intensity. Geophys. Res. Lett. 40, 5486–5491. https://doi.org/10.1002/2013GL057320
Zhou, B., Rybski, D., Kropp, J.P., 2017. The role of city size and urban form in the surface urban heat island. Sci. Rep. 7, 1–9. https://doi.org/10.1038/s41598-017-04242-2
Zhou, D., Zhao, S., Liu, S., Zhang, L., Zhu, C., 2014. Surface urban heat island in China's 32 major cities: Spatial patterns and drivers. Remote Sens. Environ. 152, 51–61. https://doi.org/10.1016/j.rse.2014.05.017
Zhao, L., Lee, X., Smith, R.B., Oleson, K., 2014. Strong contributions of local background climate to urban heat islands. Nature 511, 216–219. https://doi.org/10.1038/nature13462

Data Sources

Meridian_data, 2017

https://digimap.edina.ac.uk/webhelp/os/data_information/os_products/meridian_2.htm, data downloaded on 31st January 2017

MODIS/Terra Land Surface Temperature and Emissivity Daily L3 Global 1km Grid SIN V006 https://search.earthdata.nasa.gov/search, Data downloaded on 23rd August 2017(Earthdata, 2017). For a description of the dataset, see https://lpdaac.usgs.gov/products/mod11a1v006/

https://www.planninghelp.cpre.org.uk/planning-explained/history-of-the-planning-system, last accessed 26th September 2019.

SUPPLEMENTARY MATERIALS

Supplementary (SI)

Table S1. *Hierarchical population distribution and area for 35 biggest cities in Great Britain (50km^2 and above; source: Meridian data 2017)*

NAME OF CITY	POPULATION	AREA (km^2)
London	8519128	1,365.43
Birmingham	2273321	558.07
Manchester	2018064	506.06
Glasgow	1006585	261.85
Liverpool	792665	191.28
Sheffield	596456	164.23
Bristol	573382	135.52
Nottingham	546720	133.02
Leeds	531516	135.50
Edinburgh	472217	105.28
Leicester	429753	98.25
Newcastle Upon Tyne	420710	103.31
Portsmouth	371300	81.52
Bradford	347653	78.96
Cardiff / Caerdydd	339746	80.84
Stoke-On-Trent	323762	107.18
Bournemouth	305788	80.08
Coventry	300924	71.98
Reading	272658	78.04
Gateshead	260779	71.95
Weybridge	259047	88.69
Luton	251115	51.56
Southampton	243807	53.91
Southend-On-Sea	239424	59.37
Derby	231497	59.78
Plymouth	220942	55.91
Aldershot	214691	76.37
Northampton	198564	54.55
Milton Keynes	188643	66.86
Birkenhead	184461	53.58
Aberdeen	181027	50.27

Norwich	177619	51.98
Middlesbrough	161596	52.43
Swansea / Abertawe	150201	53.01
Telford	123416	54.26

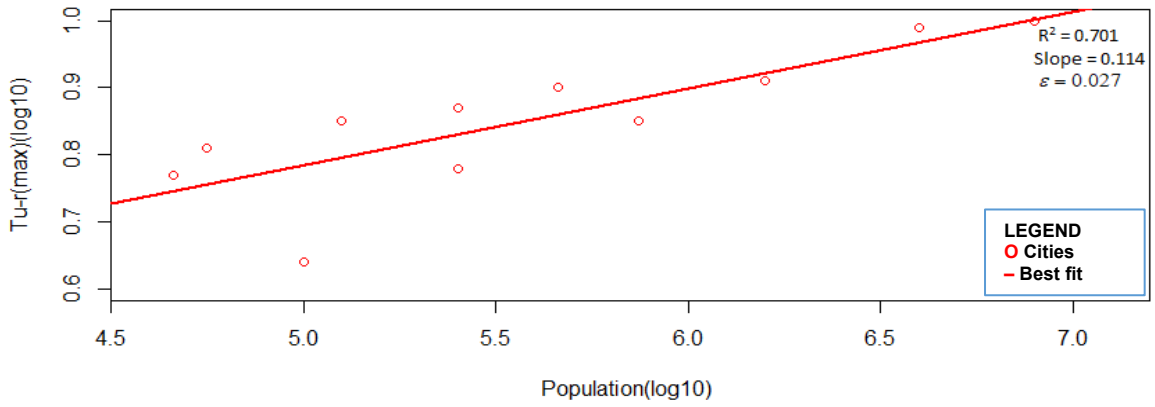

Fig. S1. *As for Figure 1 of the main text but re-drawn on log-log axes to show the power-law scaling. Reported on the graph (top right) are the Coefficient of Determination (R^2) for the best-fit regression, the slope of the regression, and the error on the slope (ε).*

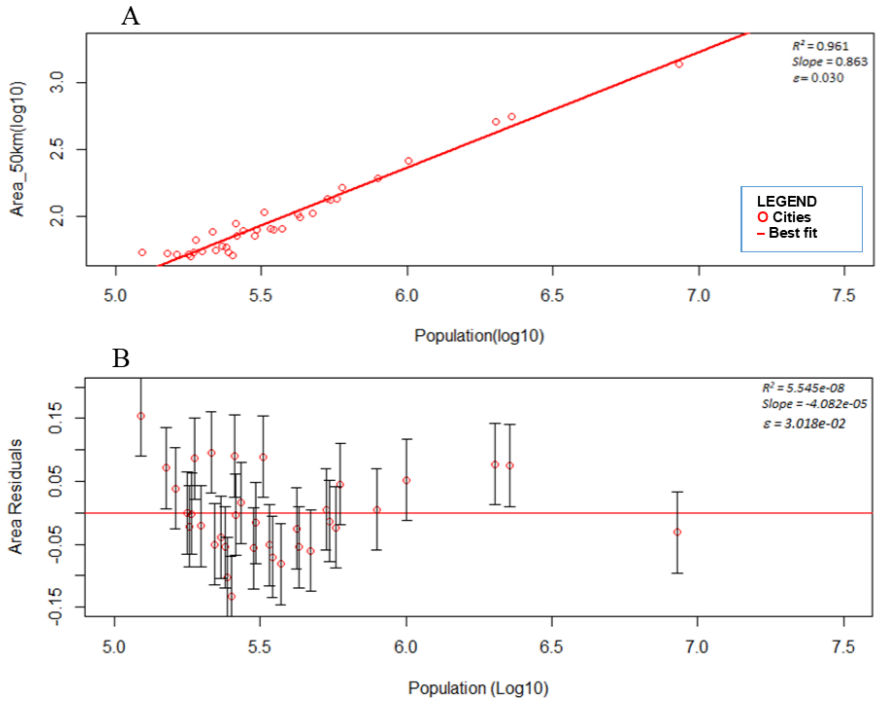

Fig. S2 (A) *Relationship between total city area and total population for 35 cities in Great Britain. The allometric regression relationship shown has a coefficient of determination (R^2 = 0.961) and*

slope = 0.86±0.03. (B) *Residuals (equation 2, main text) of city area plotted against city population. The best-fit regression values are reported but are not significant.*

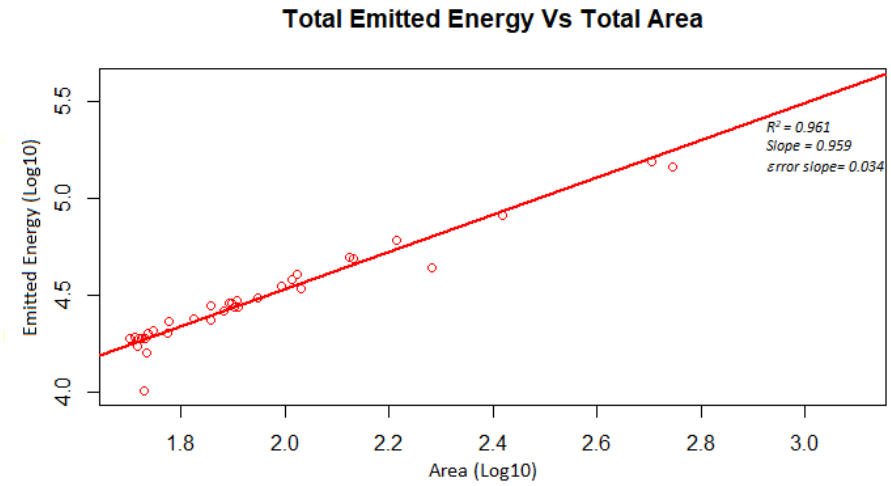

Fig S3. *Relationship between emitted energy and urban area for 35 cities in Great Britain. Reported on the graph (top right) are the Coefficient of Determination (R^2) for the best-fit regression, the slope of the regression, and the error on the slope (ε).*

Table S2. *Residuals for Emitted Energy and surface area for 35 biggest cities in Great Britain (cities are ranked by emitted energy residuals)*

NAME OF CITY	EMITTED ENERGY RESIDUAL (W m^{-2})	AREA RESIDUAL (km^2)
Telford	0.146	0.155
Stoke-On-Trent	0.086	0.089
Weybridge	0.075	0.090
Birmingham	0.074	0.075
Milton Keynes	0.073	0.087
Swansea / Abertawe	0.062	0.071
Reading	0.052	0.016
Aldershot	0.051	0.096
Glasgow	0.050	0.052
Middlesbrough	0.038	0.039
Manchester	0.038	0.078
Gateshead	0.025	-0.003
Bournemouth	0.012	-0.016
Nottingham	0.008	-0.013

Sheffield	0.001	0.045
Bristol	0.001	-0.023
Northampton	-0.002	-0.021
Leeds	-0.004	0.005
Plymouth	-0.005	-0.050
Newcastle Upon Tyne	-0.005	-0.025
Aberdeen	-0.014	-0.022
London	-0.017	-0.031
Birkenhead	-0.024	-0.001
Liverpool	-0.029	0.005
Derby	-0.030	-0.039
Cardiff / Caerdydd	-0.033	-0.051
Edinburgh	-0.046	-0.060
Norwich	-0.049	0.000
Leicester	-0.049	-0.055
Portsmouth	-0.073	-0.081
Bradford	-0.076	-0.070
Coventry	-0.077	-0.056
Southampton	-0.080	-0.103
Southend-On-Sea	-0.087	-0.054
Luton	-0.114	-0.133

853

854

855 **Table S3**. *Summary of night-time emitted energy scalings for thirty-five (35) UK large Cities on 28*
856 *selected summer and winter nights between 2000 and 2017. Results are ranked by the strength (*R^2)*
857 *of the log-log correlation between emitted energy and population, for a threshold for inclusion of a*
858 *city in the scatter plot of 75% cloud-free pixels. The table reports the allometry slope, error on slope,*
859 *intercept, and sample size at 50% and 75% cloud free pixels (*=75% cloud free pixels).*

860

861

RANK	DATE	NUMBER OF CITIES(n)	NUMBER *OF CITIES(n)	R^2	*R^2	SLOPE (α)	SLOPE *(α)	ERROR ON SLOPE (ε)	ERROR ON *SLOPE (ε)	INTERCEPT	*INTERCEPT
1	13th Feb. 2017	26	25	0.97	0.97	0.86	0.84	0.03	0.03	-0.23	-0.15
2	02nd Jan. 2017	35	33	0.94	0.97	0.84	0.83	0.04	0.03	-0.13	-0.09
3	15th Feb. 2016	25	25	0.96	0.96	0.85	0.85	0.03	0.03	-0.18	-0.18
4	06th Jun. 2000	33	32	0.96	0.96	0.85	0.88	0.03	0.03	-0.13	-0.28
5	29th Feb. 2000	21	19	0.92	0.96	0.83	0.78	0.05	0.04	-0.08	0.19
6	22nd Feb. 2003	28	28	0.96	0.96	0.88	0.88	0.04	0.04	-0.37	-0.37
7	07th Jul. 2007	34	34	0.96	0.96	0.84	0.84	0.03	0.03	-0.08	-0.08
8	01st Jan. 2007	32	32	0.96	0.96	0.85	0.85	0.03	0.03	-0.16	-0.16
9	20th Jan. 2011	22	17	0.88	0.95	0.74	0.82	0.06	0.05	0.33	-0.06
10	09th Jul. 2006	34	30	0.88	0.95	0.88	0.84	0.06	0.04	-0.31	-0.04
11	30th Aug. 2005	22	18	0.90	0.95	0.82	0.84	0.06	0.05	0.00	-0.06
12	20th Jan. 2009	18	14	0.88	0.94	0.83	0.80	0.08	0.06	-0.18	0.01
13	28th Aug. 2001	25	23	0.91	0.94	0.88	0.86	0.06	0.05	-0.30	-0.18
14	10th Jun. 2003	27	20	0.87	0.94	0.81	0.82	0.06	0.05	-0.02	-0.02
15	16th Aug. 2016	35	34	0.92	0.94	0.89	0.87	0.04	0.04	-0.31	-0.21
16	27th Jun. 2010	32	31	0.93	0.94	0.80	0.81	0.04	0.04	0.16	0.13
17	17th Dec. 2011	26	20	0.83	0.93	0.92	0.94	0.09	0.06	-0.65	-0.74
18	25th Feb. 2009	26	19	0.85	0.93	0.91	0.97	0.08	0.06	-0.62	-0.89
19	26th Dec. 2009	24	24	0.93	0.93	0.81	0.81	0.05	0.05	0.03	0.03
20	05th Jan. 2005	34	30	0.88	0.93	0.80	0.86	0.05	0.05	0.06	-0.25
21	13th Jul. 2002	28	22	0.87	0.92	0.77	0.80	0.06	0.05	0.22	0.14
22	30th Nov. 2016	20	17	0.92	0.92	0.86	0.82	0.06	0.06	-0.30	-0.08
23	18th Feb. 2006	25	23	0.79	0.92	0.84	0.86	0.09	0.06	-0.15	-0.21
24	01st Jan. 2012	24	24	0.92	0.92	0.89	0.89	0.06	0.06	-0.43	-0.43
25	08th Aug. 2012	25	20	0.88	0.89	0.83	0.99	0.06	0.08	-0.07	-0.95
26	03rd Aug. 2017	22	18	0.86	0.86	0.82	0.84	0.07	0.09	-0.06	-0.17
27	13th Dec. 2010	17	15	0.92	0.84	0.73	0.91	0.06	0.11	0.35	-0.62
28	28th Aug. 2009	30	21	0.84	0.82	0.81	0.88	0.07	0.09	-0.02	-0.36
	Mean					0.84	0.86	0.06	0.05	-0.13	-0.22
	Median					0.83	0.85				

Table S4. *Summary of night-time emitted energy for UK large Cities with populations* ***>250,000 and >500,000*** *on selected summer and winter nights. Results are ranked by the strength (R^2 [@50%]) of the log-log correlation between emitted energy and population, for which the slope, error on slope, and intercept are reported*

RANK	DATE	NUMBER OF CITIES (n)	NUMBER OF CITIES *(n)	R^2	*R^2	SLOPE (α)	SLOPE *(α)	ERROR ON SLOPE (ε)	ERROR ON SLOPE *(ε)	INTERCEPT	*INTERCEPT
1	15th Feb. 2016	16	7	0.98	0.99	0.86	0.85	0.04	0.04	-0.23	-0.19
2	13th Feb. 2017	16	7	0.97	0.97	0.82	0.84	0.04	0.06	-0.02	-0.10
3	16th Aug. 2016	22	9	0.97	0.98	0.87	0.89	0.03	0.04	-0.22	-0.32
4	07th Jul. 2007	22	9	0.97	0.98	0.85	0.86	0.03	0.05	-0.13	-0.16
5	01st Jan. 2007	21	8	0.97	0.98	0.85	0.87	0.04	0.06	-0.17	-0.30
6	29th Feb. 2000	15	7	0.97	0.96	0.81	0.78	0.04	0.07	0.03	0.24
7	02nd Jan. 2017	22	9	0.96	0.96	0.83	0.84	0.04	0.06	-0.07	-0.14

8	06th Jun. 2000	21	8	0.96	0.96	0.83	0.82	0.04	0.07	-0.02	0.06
9	22nd Feb. 2003	19	8	0.95	0.98	0.88	0.87	0.05	0.05	-0.35	-0.27
10	28th Aug. 2001	15	4	0.95	0.99	0.89	0.84	0.06	0.07	-0.38	0.01
11	09th Jul. 2006	22	9	0.95	0.95	0.82	0.85	0.04	0.08	0.05	-0.15
12	30th Nov. 2016	11	2	0.95	1.00	0.90	0.84	0.07	NA	-0.52	-0.10
13	26th Dec. 2009	13	5	0.94	0.98	0.84	0.92	0.07	0.07	-0.14	-0.68
14	01st Jan. 2012	16	7	0.93	0.95	1.02	0.98	0.07	0.10	-1.15	-0.93
15	13th Dec. 2010	10	5	0.92	0.93	0.66	0.58	0.07	0.09	0.81	1.31
16	05th Jan. 2005	21	9	0.92	0.90	0.81	0.65	0.05	0.08	0.03	1.01
17	27th Jun. 2010	20	8	0.92	0.95	0.81	0.87	0.06	0.08	0.14	-0.25
18	20th Jan. 2011	16	7	0.90	0.98	0.69	0.55	0.06	0.04	0.66	1.52
19	30th Aug. 2005	15	6	0.90	0.94	0.79	0.88	0.07	0.11	0.18	-0.38
20	20th Jan. 2009	12	4	0.89	0.88	0.90	0.85	0.10	0.22	-0.58	-0.29
21	03rd Aug. 2017	14	6	0.87	0.83	0.85	0.74	0.09	0.17	-0.21	0.47
22	28th Aug. 2009	20	8	0.87	0.92	0.88	0.80	0.08	0.09	-0.43	0.12
23	10th Jun. 2003	16	6	0.87	0.93	0.83	0.97	0.09	0.13	-0.11	-0.99
24	08th Aug. 2012	17	7	0.87	0.84	0.84	0.85	0.08	0.16	-0.16	-0.20
25	13th Jul. 2002	15	5	0.86	0.99	0.79	1.00	0.09	0.05	0.13	-1.20
26	25th Feb. 2009	16	7	0.85	0.88	1.02	0.93	0.11	0.16	-1.27	-0.72
27	18th Feb. 2006	16	6	0.82	0.98	1.02	0.98	0.13	0.08	-1.20	-0.92
28	17th Dec. 2011	16	6	0.79	0.76	0.92	0.83	0.13	0.23	-0.67	-0.12
	Mean					**0.85**	**0.84**	**0.07**	**0.09**	**-0.21**	**-0.13**
	Median					**0.84**	**0.85**				

871 * = Population >500,000

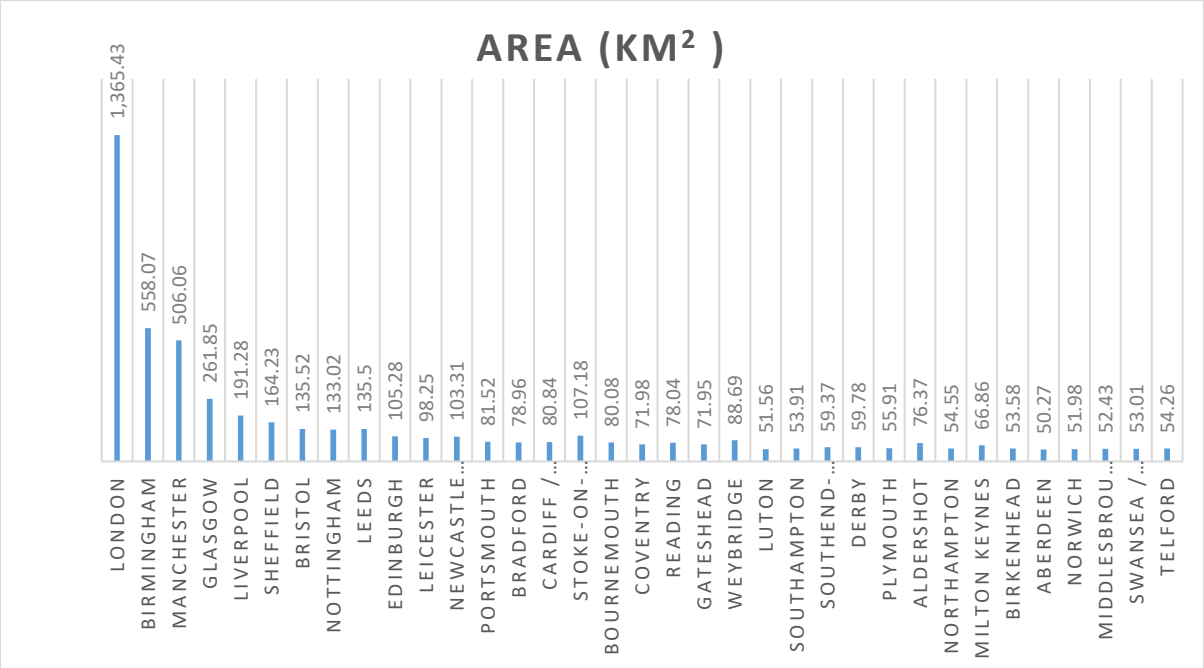

872

873 **Fig. S4** *Hierarchical Area distribution for the 35 biggest cities in Great Britain*

874

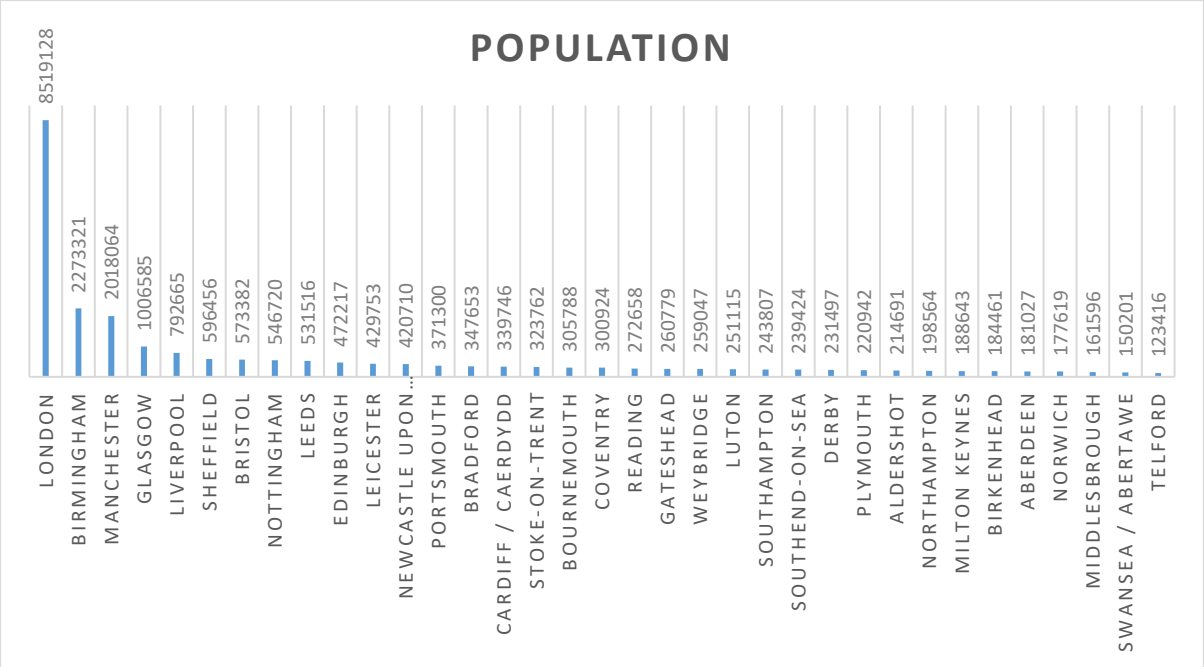

Fig. S5 *Hierarchical population distribution for the 35 biggest cities in Great Britain*

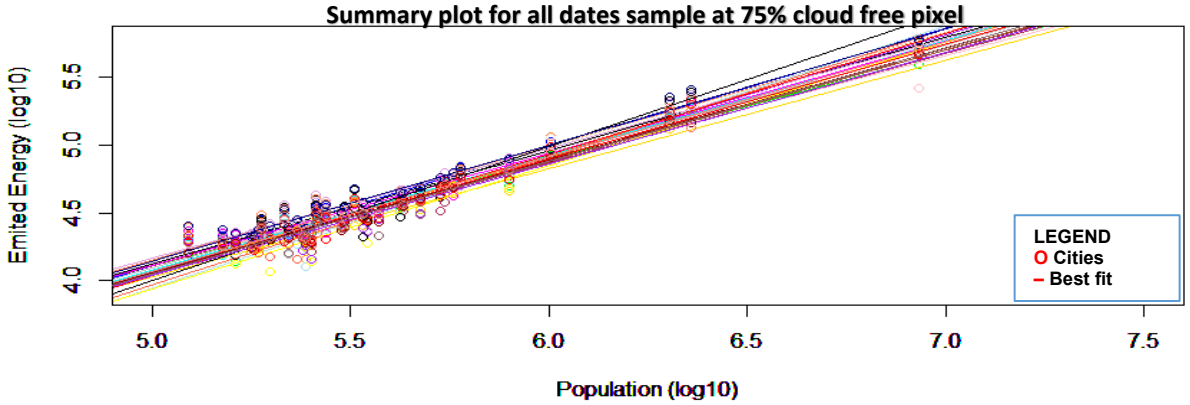

Fig. S6 *Relationship between total emitted energy and total population across Cities in Great Britain for selected nights, listed in Table 3. Each colour represents a different night. Allometric regressions are plotted for each night, the equations for which are reported in Table 3. The overall best straight line through the data is* ***0.86±0.05.***

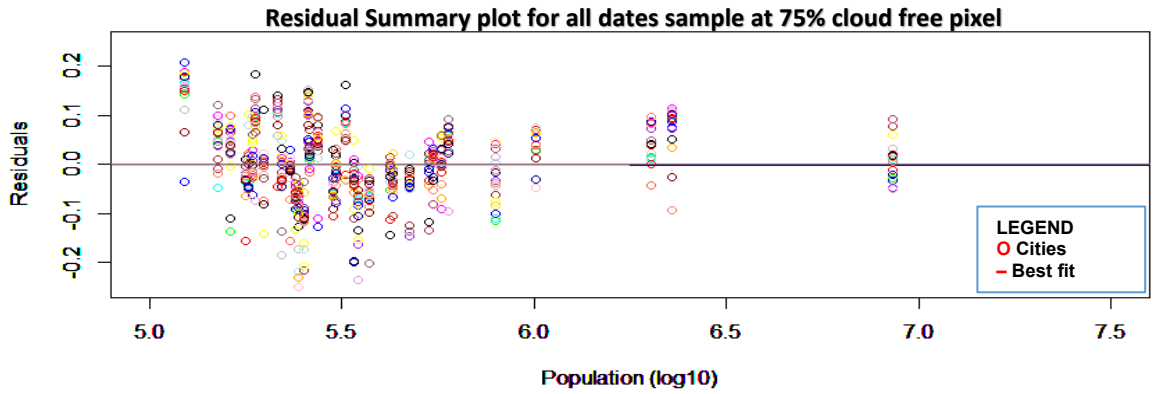

885
886 **Fig. S7** *Residual Summary plot for all dates sample at 75% cloud free pixel*

887

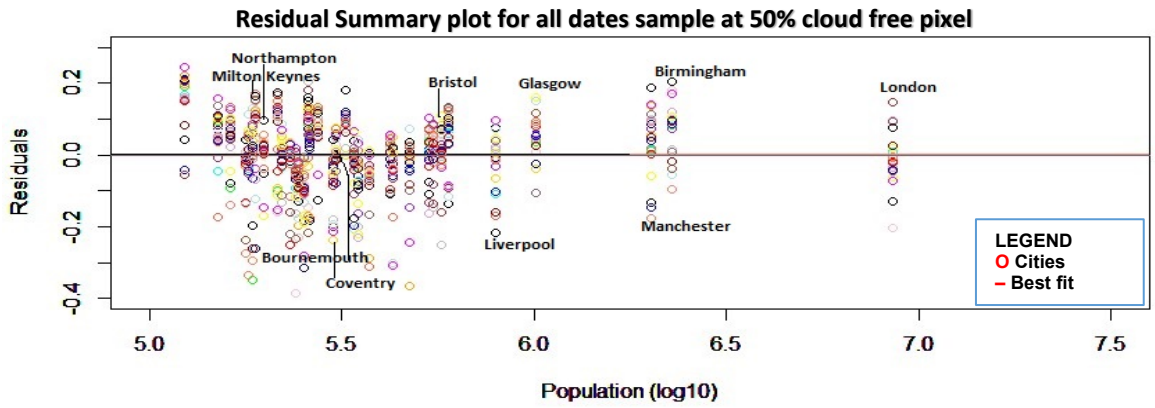

888
889 **Fig. S8** *Residual Summary plot for all dates sample at 50% cloud free pixel*

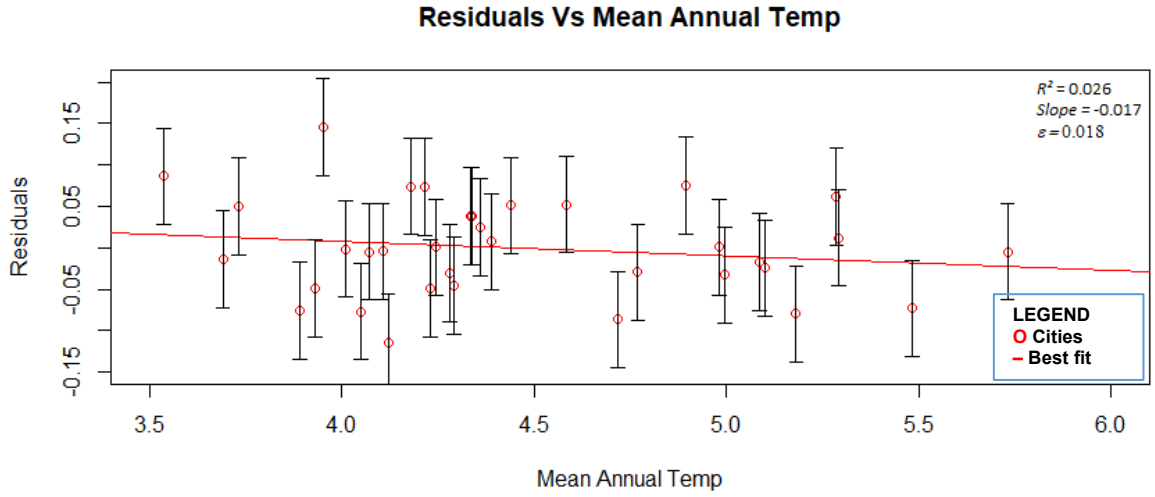

890
891 **Fig. S9** *Mean Residuals plots Vs Mean Annual Temperature*

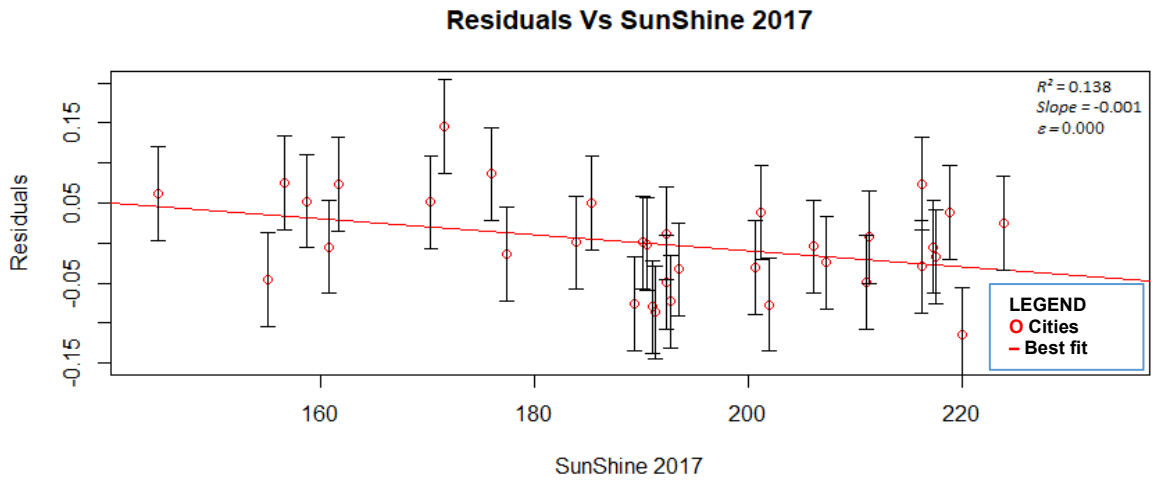

892
893 **Fig. S10** *Mean Residuals plots Vs Hours of Sunshine*

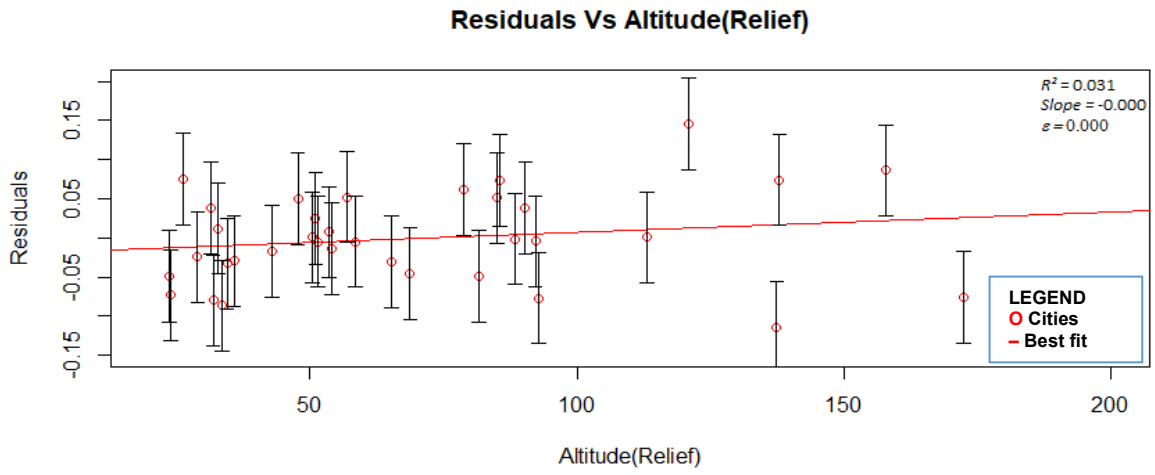

894
895 **Fig. S11** *Mean Residuals plots Vs Altitude*

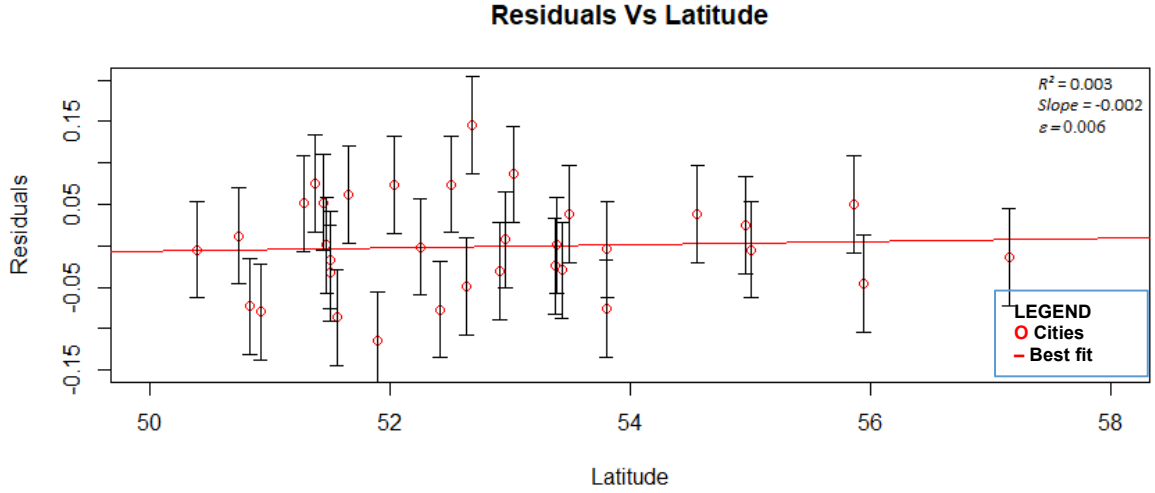

896

Fig. S12 *Mean Residuals plots Vs Latitude. The regression is not significantly different from zero and explain 0.3% of the variance.*